

A STUDY OF OPERATIONAL VARIABLES INFLUENCING WHEEL
BALANCING MEASUREMENTS.

by

Aneesh Nabar

A thesis submitted to the faculty of
The University of North Carolina at Charlotte
in partial fulfillment of the requirements
for the degree of Master of Science in
Mechanical Engineering

Charlotte

2016

Approved by:

Dr. Peter T. Tkacik

Dr. Mesbah Uddin

Dr. Christopher Vermilion

© 2016
Aneesh Nabar
ALL RIGHTS RESERVED

ABSTRACT

ANEESH NABAR. A study of operational variables influencing wheel balancing measurements.

(Under the direction of DR. PETER T. TKACIK)

The aim of this research is to analyze various operational parameters that may affect the wheel balancing measurement. Therefore, wheel balancing measurements were taken iteratively on different low profile wheel/tire assemblies for different conditions to understand which operational conditions influence the measurements. These low profile tires include 205/50 ZR 17 89Y, 265/35 ZR 18 (97 Y), 225/40 ZR 18 (97Y), 265/35 R18 (97 Y), 265/35 R18 (97Y), 205/40 R17 84H, 255/40 ZR 17 94(Y). The measurements were taken on Hunters wheel balancing machine - DSP9200.

Accuracy and repeatability of the existing machine was determined using statistical methods. Repeatability and accuracy of the measurements for one particular set of readings were confirmed by clocking (Dismounting tire from machine and rotating at certain degrees and re-mounting it) the tire 45 degrees after every two measurements. Based on the knowledge of wheel balancing operations, a mathematical equation was deduced and error analysis of this equation based on the dependent variables was performed. A custom adapter to mount the wheel on wheel balancer was designed to improve centering of the wheel on the spindle shaft to enhance the precision of the wheel balancer. High end cars such as Porsche or Mercedes are equipped with high-performance wheels. These high performance tires are rated for speed of 185 mph and above. A slight imbalance on the wheel assembly of these cars may considerably affect the vehicle ride. Hence the special adapter was designed for high performance tires of Porsche. Wheel balancing machine's repeatability was improved considerably after replacing the conventional wheel mounting cone spacer with the newly designed adapter.

Finally, ways to improve the design of the wheel mounting adapter and a method for better calibration of the machine are discussed in the scope for future work.

DEDICATION

To my parents Kiran and Jayashree Nabar, sister Pooja and my grandparents Vasudeo and Suchita Nabar for their motivation, love and support throughout this journey.

ACKNOWLEDGEMENTS

I would like to begin by thanking my advisor, Dr. Peter T. Tkacik, for his constant guidance and motivation. He made this project a great learning experience for me. Without his support, this thesis would not have been possible.

I would like to thank Dr. Mesbah U. Uddin and Dr. Christopher Vermilion for their help and suggestions, and also for being on the committee for this project.

I would also like to thank Mr. Luke Woroneicki and Mr. Kile Stinson for their help in getting the special wheel mounting adapter manufactured and helping me get acquainted with necessary equipment and also for their help in acquiring and validating the results.

A special appreciation for my fellow students, Harsh Patel, Jugal Popat for their help and unique inputs time to time.

I would also like to thank all of my dear friends who were like a family to me. Their support and motivation throughout this journey has been very helpful.

Lastly I would like to thank the Mechanical Engineering Department, College of Engineering for providing state-of-the-art research facilities at Motorsport Research Building.

LIST OF FIGURES	ix
LIST OF TABLES	xii
CHAPTER 1: INTRODUCTION	1
1.1 Wheel Balancing	1
1.2 Types of Wheel Balancing Systems	2
1.3 Influence of Wheel Balancing on Vehicles Performance	2
1.4 Scope of Study	3
1.5 Organization of Thesis	3
CHAPTER 2: LITERATURE REVIEW	4
2.1 Vibrational Behavior of Imbalanced Tire	4
2.2 Wheel Balancing Machine	5
2.3 Wheel Balancing Weight	16
2.3.1 Type of Wheel Weights	17
2.3.2 Hammer-on Weights	19
2.3.3 Tape-on Weights	22
2.3.4 Curvature Effect of Wheel Balancing Weight	25
2.4 Calibration of the Apparatus and Improvement of Imbalance Determination	26
2.4.1 Wheel Balancer Quick Calibration Check	26
CHAPTER 3: MATHEMATICAL EQUATION OF WHEEL BALANCING OPERATION	32
3.1 Mathematical Equation of Wheel Balancing	32
3.2 Error Analysis of Wheel Balancing Equations	36
3.2.1 Error Analysis of m_1	37
3.2.2 Error Analysis of m_2	39

CHAPTER 4: METHODOLOGY	42
4.1 Test Wheels and Wheel Conditions	42
4.2 Introduction to Hunter DSP9200 Wheel Balancer	44
4.2.1 Balancing Overview	46
4.2.2 Balancing Wheel on DSP9200 and Various Features of The Machine	49
4.3 Centering of Wheel on Wheel Balancer	52
4.3.1 Design and Manufacturing of Wheel Balancer Adapter	54
4.4 Test Protocol	58
4.5 Procedure	62
CHAPTER 5: RESULTS AND DISCUSSION	68
5.1 Test Protocol 1: Effect of Pressure	68
5.2 Test Protocol 2: Effect of Clocking	70
5.3 Test Protocol 3: Effect of Tightening Torque	74
5.4 Test Protocol 4: Effect of Wheel Offset	75
5.5 Test Protocol 5: Axial Sensitivity of Dataset Arm	78
5.6 Test Protocol 6: Radial Sensitivity of Dataset Arm	80
5.7 Test Protocol 7: Performance of Specially Designed Wheel Mounting Adapter	81
CHAPTER 6: CONCLUSION AND FUTURE SCOPE	86
6.1 Conclusion	86
6.2 Future Scope	87
BIBLIOGRAPHY	89

FIGURE 2.1: Top view of wheel balancer spindle shaft assembly	6
FIGURE 2.2: Schematic electrical diagram of wheel balancer	8
FIGURE 2.3: Force computer's electrical circuit	9
FIGURE 2.4: Count pulse circuit	14
FIGURE 2.5: Installation of hammer-on weight	17
FIGURE 2.6: Hammer-on weight clip profile	18
FIGURE 2.7: Cross section of wheel with hammer-on weight applied	20
FIGURE 2.8: Cross section of hammer-on weights	21
FIGURE 2.9: Tape-on type wheel balancing weight	23
FIGURE 2.10: Detailed drawing of tape-on weight	24
FIGURE 2.11: Curvature effect of balancing weight	26
FIGURE 2.12: Quick calibration mode	28
FIGURE 2.13: Flowchart for calibration check	30
FIGURE 3.1: Force transducer and encoder assembly on spindle shaft	32
FIGURE 3.2: Imbalance forces in wheel plane	33
FIGURE 3.3: Force transducer and encoder assembly on spindle shaft	34
FIGURE 4.1: Wheel balancer DSP9200 with pointing laser	44
FIGURE 4.2: Components of wheel balancer DSP9200	46
FIGURE 4.3: Static imbalance	47
FIGURE 4.4: Dynamic imbalance	48

FIGURE 4.5: Dynamic balance weight planes	49
FIGURE 4.6: Wheel mounting assembly	50
FIGURE 4.7: Wheel mounting adapter model	56
FIGURE 4.8: Assembly of wheel mounting adapter with wheel rim and spindle shaft	57
FIGURE 4.9: Wheel mounting adapter after manufacturing	58
FIGURE 4.10: Reference markings on wheel rim and wheel balancer flange	60
FIGURE 4.11: Close-up of reference marking	60
FIGURE 4.12: Method to calculate tightening torque	60
FIGURE 4.13: Offsetting wheel mounting cone with metal shims	61
FIGURE 4.14: Wheel calibration	64
FIGURE 4.15: Laser pointer mounted on wheel balancer	65
FIGURE 4.16: Wheel calibration and laser pointer close up	65
FIGURE 4.17: Calibration of the machine	66
FIGURE 5.1: Test tire:225/40ZR18 - effect of pressure on balancing weight	69
FIGURE 5.2: Test tire:225/40ZR18 - effect of pressure on location of balancing weight	69
FIGURE 5.3: Test tire:265/35ZR18 - effect of pressure on balancing weight	70
FIGURE 5.4: Test tire:265/35ZR18 - effect of pressure on location of balancing weight	71
FIGURE 5.5: Test tire:225/40ZR18 - effect of clocking on balancing weight	71
FIGURE 5.6: Test tire:225/40ZR18 - effect of clocking on location of balancing weight	72
FIGURE 5.7: Test tire:255/40ZR17 - effect of clocking on balancing weight	72

FIGURE 5.8: Test tire:255/40ZR17 - effect of clocking on location of balancing weight	72
FIGURE 5.9: Test tire:205/40ZR17 - effect of clocking on balancing weight for four revolution	73
FIGURE 5.10: Test tire:205/40ZR17 - effect of clocking on location of balancing weight for four revolution	73
FIGURE 5.11: Test tire:265/35ZR18 - effect of tightening torque on wheel balancing measurements	74
FIGURE 5.12: Test tire:225/40ZR18 - effect of tightening torque on wheel balancing measurements	75
FIGURE 5.13: Test tire:225/40ZR18 - effect of offsetting wheel with metal shims of different thickness	76
FIGURE 5.14: Test tire:225/40ZR18 - variation in balancing weight while using 0.06 mm thick metal shim offset	77
FIGURE 5.15: Test tire:225/40ZR18 - variation in location of balancing weight while using 0.06 mm thick metal shim offset	78
FIGURE 5.16: Test tire:225/40ZR18 - effect of offsetting inner dataset arm	79
FIGURE 5.17: Test tire:225/40ZR18 - effect of offsetting outer dataset arm	80
FIGURE 5.18: Test tire:225/40ZR18 - effect of offsetting dataset arm radially	81
FIGURE 5.19: Test tire:225/40ZR18 - measurements with new adapter, clocking wheel and adapter together	82
FIGURE 5.20: Test tire:225/40ZR18 - measurements with new adapter, clocking wheel alone	83
FIGURE 5.21: Test tire:265/35ZR18 -measurements with new adapter, clocking wheel and adapter together	84
FIGURE 5.22: Test tire:265/35ZR18 - measurements with new adapter, clocking wheel alone	85

LIST OF TABLES

TABLE 4.1: Designation of the test wheels	43
TABLE 4.2: Hunter DSP9200 wheel balancer specifications	45

CHAPTER 1: INTRODUCTION

The automotive wheel is the only contact point between vehicle and road. The power generated by the automotive engine is transferred to wheels by means of transmission and drive shafts. Considering the average speed of passenger vehicle to be 60 mph and wheel diameter to be 2 feet, hence, on an average, the automotive wheel turns 840 revolutions per minute (14 revolutions per second). At such a high speed even one ounce of imbalance present in the wheel can cause vibration on the wheel as well as steering to a great extent. Modern day car has very sensitive steering wheel, which gives driver feel of even slight vibration in the wheel. In spite advance manufacturing process new tire does have some amount of imbalance which needs to be compensated for. Hence balancing an automotive wheel is truly important.

1.1 Wheel Balancing

A wheel balancing system is used to reduce vibrations in out-of-balance automotive wheel and tire assembly by placement of corrective balancing weights to wheel assembly. Typically, combined tire and wheel assembly is mounted on a rotatable shaft of wheel balancer which includes forces transducer connected to reliably supported bearings for the shaft which calculates the amount of imbalance in the wheel and tire assembly. Encoders are included to locate the position of imbalance force thus using this information machine calculates the position where corrective weight needs to be attached. Wheel balancing can be broadly classified into two types: 1) Static Balance and 2) Dynamic Balance [1]

1.2 Types of Wheel Balancing Systems

Wheel balancing can be broadly classified into two types: 1] Static Balance and 2] Dynamic Balance

Static Balance: In Static balancing the tire and wheel assembly is considered as a single plane and is not spinning. In static wheel balancing combined wheel and tire assembly is mounted on a vertical spindle tool. The gravitational pull acting on the imbalance mass causes the tool to bend down. The amount of deflection in the vertical tool indicates the magnitude of the imbalance weight. The deflection angle indicates the angular position of imbalance weight on the wheel. Thus corrective weights are applied accordingly. In tire manufacturing factory, for more accuracy, sensors are employed on spindle tool to get the magnitude and position of imbalance weight whereas in retail shops oil filled, center bubble level gauge is used. [2]

Dynamic Balance: When the wheel is rotated at high speed imbalance weight generates centrifugal force and causes wheel assembly to wobble. When the tire is rotated at high speed, the forces generated by asymmetric weight distribution is described as dynamic balance. In dynamic balance wheel is resolved into two planes, inner and outer, where corrective weights are to be attached. The wheel is rotated at high speed on dynamic wheel balancer and unbalanced forces are measured by force transducer as the wheel rotates. Static imbalance forces are calculated for inner and outer planes and couple imbalance of these two is calculated for dynamic wheel balance. Corrective balancing weights are then attached to inner and outer planes, that is, inner and outer edge of the wheel rim. Dynamic balancing is more comprehensive as it accounts for both static as well as couple imbalance. [2]

1.3 Influence of Wheel Balancing on Vehicles Performance

The presence of an imbalance in wheel/tire assembly is very much inevitable. When an out-of-balance wheel rotates at high speed, imbalance spot on the wheel generates centrifugal force. Imbalance forces on wheel causes wheel to vibrate and vibrations become progressively worse as vehicle's speed increases. Minimum vehicle

speed at which vibrations can be experienced depends on the size and weight of the tire-wheel assembly, magnitude and location of imbalances force, size and weight of the vehicle and sensitivity of steering wheel. Vibrations from wheel assembly transmit to suspension thereby deteriorating the ride quality. This, in turn, will also reduce fuel economy. Out-of-balance wheel will increase tire wear and increase in tire wear will make the balance of wheel even worse. Considering all these troubles balancing wheel periodically is important.

1.4 Scope of Study

As learned from section 1.3, wheel balancing is of utmost important. It is, therefore, important to make the balancing measurements accurately. This being the motivation of the study following parameters will be evaluated in this research: I. Effect of operator variables on wheel balancing II. Effect of wheel condition variables III. Effect of apparatus condition

1.5 Organization of Thesis

Chapter 1 introduces the reader to need of wheel balancing and techniques used. This chapter also indicates the scope and motivation of this study. Chapter 2 explains working of wheel balancing machine and elaborates more on balancing techniques. Calibration of the machine is also discussed. Chapter 3 dives in the mathematical equations of working of wheel balancing machine and also covers error analysis of these equations. Chapter 4 test protocol for the wheel balancing measurements carried out in this study is explained in this chapter. Design of new wheel mounting adapter is also discussed in this chapter. Chapter 5 enlists results of various tests. Chapter 6 concludes the topic and discusses about future scope in this research.

CHAPTER 2: LITERATURE REVIEW

In a modern world, automobiles are an integral part of our life. Automobile's performance not only depends on the power that its engine generates but also is equally dependent on the dynamic performance of the vehicle. Dynamic performance of the vehicle is greatly influenced by tire characteristics and tire performance. A perfectly balanced tire/wheel assembly can improve vehicle ride quality substantially as compared to vehicle's performance with an imbalanced tire. As discussed in the introduction, for better vehicle performance and life as well as passenger's comfort it is important to balance wheel periodically.

2.1 Vibrational Behavior of Imbalanced Tire

There are four major factors that induce tire noise and vibrations; tire imbalance, tire non-uniformity, tread pattern design and tire cavity resonance. As this study is confined to wheel balancing, the only vibration due to tire imbalance will be discussed here. [3]

Imbalance can be of two types; static and dynamic. Static or in-plane, imbalance causes periodic force variation at wheel axle in vertical and longitudinal directions. Common sources for tires static imbalance are large splice, multiple splices near the same area or non-uniform mass distribution due to manufacturing defects or tire wear. The non-symmetrical axis of rotation can also be a cause of static imbalance in the tire. The magnitude of the imbalance can be calculated with the equation written below. [3]

$$F = M * \omega^2 * r \quad (2.1)$$

Where,

$F = \text{Imbalance force}$

$M = \text{Imbalance mass}$

$r = \text{Effective radius}$

$\omega = \text{Angular velocity}$

Non-symmetric mass distribution along the rotational axis causes dynamic imbalance. Dynamic imbalance produces aligning moment variation along the vertical axis and overturning moment variation along the longitudinal axis. Dynamic imbalance can cause vibrations in steering wheel assembly, which makes it particularly important to have a tire mounted on steered wheel to be balanced. [3]

2.2 Wheel Balancing Machine

Apparatus used for detecting and correcting the imbalance in tire/wheel assembly is called wheel balancing machine. A typical wheel balancer includes force transducers positioned in a plane perpendicular to the rotatable shaft onto which wheel is mounted. These transducers are placed against resiliently supported bearings for the shaft to detect imbalance force created by the out-of-balance wheel.

In the dynamic balancing of a motor wheel, measurements can directly be taken on the wheel running on a vehicle, or the wheel can be taken out from the vehicle and mounted on wheel balancer shaft and then rotated. When out-of-balance wheel mounted on the drive shaft is rotated, the imbalance forces cause the drive shaft to rotate slightly off-axis in measuring plane. Force transducer attached in measuring plane provide a signal which is equivalent in a magnitude of imbalance weight. The location of imbalance force is then determined by the encoders with respect to the planes through the inner and outer rim of the wheel. The corrective balancing weight

is then attached to inner and outer plane of the wheel on the locations provided by the transducer. [4]

Brief description of the apparatus:

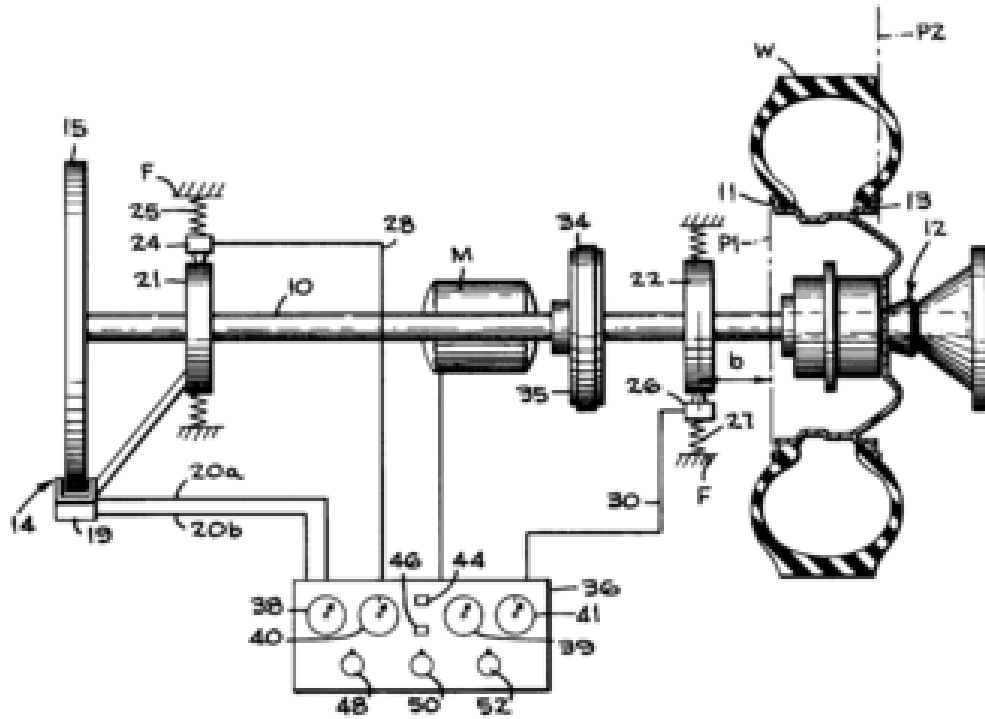


Figure 2.1: Top view of wheel balancer spindle shaft assembly [4]

Figure 2.1 is a diagrammatic top view of the wheel balancing apparatus. The apparatus, as shown above, includes a shaft (no 10) to rotate the wheel and clamping assembly 12 at one end to attach wheel firmly to shaft as it rotates. An assembly of encoder disc and optical switch (no 14) is fixed at the end of shaft opposite from where the wheel is mounted. This assembly produces analog signal outputs on 20a and 20b lines. These signals are representative of the amount of angular rotation of shaft 10. Shaft rotates freely in resiliently mounted pair of bearing spaced axially in housing 21 and 22 in a manner that is can deflect in horizontal plane if acted upon by imbalance force produced by wheel W. Transducers, 24 and 26 are placed between

bearing housing 21, 22 and a fixed frame F. Transducer give out signal 28 and 30 representing magnitude of imbalance force exerted by shaft on bearing housing 21, 22 respectively. Shaft 10 is connected to driving electric motor M through pulley 35 and belt 34 connection. The motor is situated directly below the shaft. [4]

Console board 36 includes all the switches, dials and meters to control and monitor wheel balancer. The magnitude of corrective weight that is to be attached to inner rim position 11 of wheel W is displayed on weight meter 38 and angular position of corrective weight is displayed on meter 40. Similarly, meter 39 and 41 are used to display magnitude and position of corrective weight on outside rim position 13. Dial 48 displays diameter of the wheel W. 48 provides the diameter of the wheel whereas 50 provides the width of the rim. Dial 52 provides offset distance from plane P1 to transducer 26. The dial 48, 50 and 52 are set by the operator manually prior to the start of balancing operation. [4]

A vertical leaf spring supports bearing housing 21 and 22 resiliently which allows bearings, shaft and drive pulley to deflect in horizontal plane as it is subjected to imbalance centrifugal force produced by the imbalanced wheel W. Transducers 24 and 26 contains piezoelectric crystal device placed in between respective bearing housing and fixed frame F. Spring 25 and 27 are used between frame and transducer to maintain force measuring contact. These transducers are placed in horizontal plane matching the shaft's centerline thus produces a sine wave signal proportional to horizontal components of the imbalance force generated by the out-of-balance wheel.

As shown in figure 2.2 signal outputs of the transducer device 24 and 26 are transferred to force computer 56 (which is shown in details is figure 2.3) which generates sinusoidal wave and transfer to line 58a and 58b. Output signals on 58a and 58b indicate the magnitude and location of corrective imbalance weight to be attached to inner and outer planes of rim P1 and P2 respectively. As transducers are placed in the horizontal plane and deflection of bearing housing is restricted in the horizontal

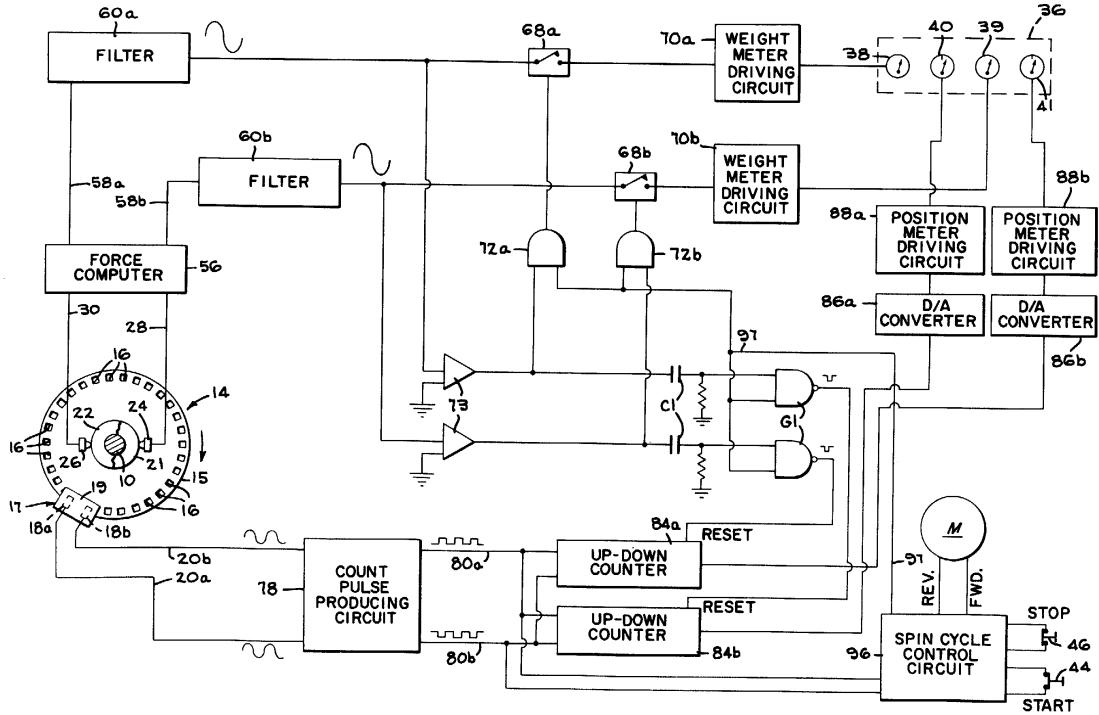


Figure 2.2: Schematic electrical diagram of wheel balancer [4]

plane, the (imbalanced weight) heavy spot on the plane P1 and P2 will be at the bottom dead center of rim 11 and 13 when the phase angle is 180 degrees on lines 58a and 58b respectively. Corrective weight position at this case will be on the top dead center. Top dead center position for emplacement of corrective weight is chosen as it the most convenient place to put on the weights. [4]

The transducer measures forces in the plane of bearing housings 21 and 22. To compute the imbalance force acting in the plane P1 and P2 of wheel W, following equation can be used,

$$W_2 = a/c * F_1 + b * [F_1 F_2]/c \quad (2.2)$$

$$W_1 = F_2 - F_1 - w_2 \quad (2.3)$$

Where,

W_1 = magnitude of imbalance force in plane P1 effective at rim 11.

W_2 = magnitude of imbalance force in plane P2 effective at rim 13.

F_1 = horizontal force acting on transducer 24 exerted by oscillating and rotating shaft 10.

F_2 = horizontal force acting on transducer 26 exerted by oscillating and rotating shaft 10

a = axial distance between two transducers

b = axial offset of transducer 26 and plane P1

c = width of wheel W

Since W_1 and W_2 are the values of force acting in plane P1 and P2, therefore, amount of weight that is needed to be applied on the counter-balance position is calculated by dividing force by rim radius, that is W_1/r and W_2/r for planes P1 and P2 [4]. This equations are explained in details in chapter 3.

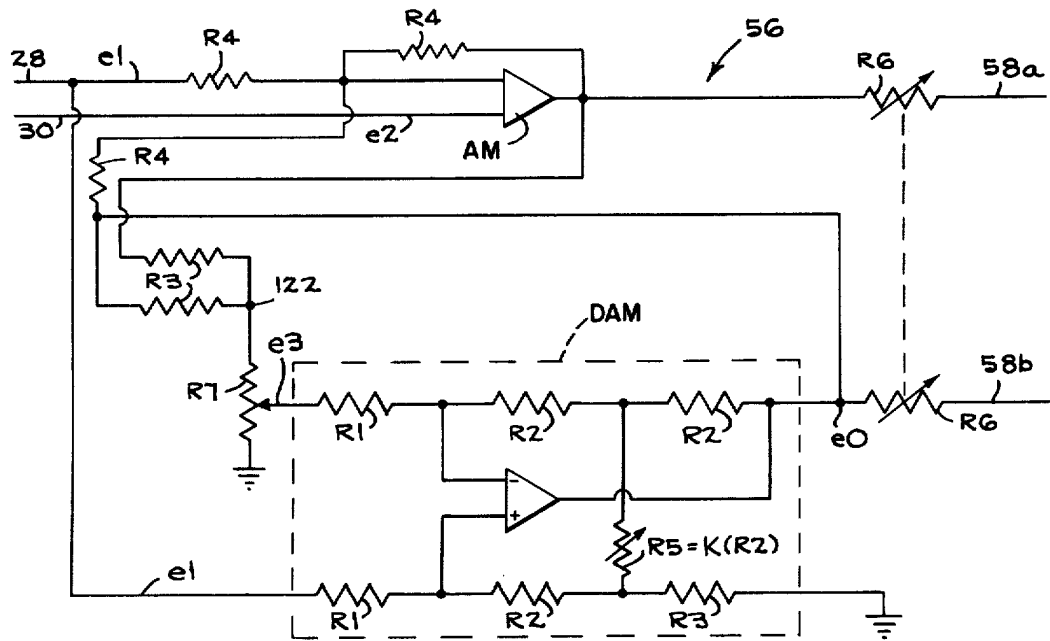


Figure 2.3: Force computer's electrical circuit

[4]

Figure 2.3 describes the detailed circuit for force computer 56 which accomplishes calculations according to equations 2.2 and 2.3. The first stage of force computer, as shown in figure 2.3, includes an amplifier 'AM'. The non-inverting terminal of this amplifier is connected to line 30 coming from transducer 26. Line 30 supplies non-inverting end of AM with voltage e_2 which is representative of force F_2 exerted by the shaft on transducer 26. Inverting end of amplifier AM is connected to line 28 coming from transducer 24 which supplies AM with voltage e_1 , representative of force F_1 exerted by the shaft on transducer 24. The second stage of force computer 56 has output voltage e_0 , which corresponds to W_2 force value. Refer to equation 2.3 above. The output of amplifier AM is equivalent to force value of W_1 . This is value is applied to settable variable resistance R_6 proportional to radius r of the wheel. Therefore, the signal provided by it is the representation of the corrective weight to be attached to rim 11. Resistance value R_6 can be set by dial 48. The second stage of force computer 56 is adjustable gain differential amplifier denoted by DAM. The gain of DAM is controlled by a variable resistor $R = K(R_2)$, where the value of K is set by wheel width dial 50. DAM includes two matched resistors R_1 and four matched resistors R_2 as shown in figure 2.3 The output voltage e_0 of this amplifier is given by the following equation [4]:

$$e_0 = 2(1 + 1/K) * (R_2/R_1) * (e_1 - e_3) \quad (2.4)$$

The non-inverting terminal input voltage of differential amplifier DAM is equivalent to force F_1 . The output from differential amplifier DAM is fed back to one of the matched resistor R_3 and summed at point 122 with amplifier AM's output through other matched resistor R_3 . The output voltage of point 122 is passed through potentiometer R_7 , the value of which is set by the offset distance b' . Voltage e_3 is output after pot R_7 . e_3 voltage is applied to the inverting terminal of differential amplifier DAM. When the potentiometer R_7 is set to a non-zero value, the input voltage e_3

applied to the inverting terminal of DAM will be of a value set by potentiometer $R7$. Output voltage e_0 of DAM will be a function of wheel width K set by resistor $R5$. [4]

As it can be seen in figure 2.2 output signal from force computer 56 are passing through line 58a and 58b are applied to filters 60a and 60b which are tuned to the frequency of tire rotation during the wheel balancing test to provide miscellaneous noise free sine wave signal. The most suitable filter in this case is standard multi-pole, narrow-band pass filter. It is required that shaft is rotating at a fixed speed when fixed frequency filter is used. Outputs of filters 60a and 60b are passed through monostable switch 68a and 68b and are applied to weight meter driving circuits 70a and 70b respectively. Switching circuits 68a and 68b are energized by output from a pair of AND gates 72a and 72b. Output from these two AND gates will be high to close monostable switches 68a and 68b, as the positive half of the signal from force filter 60a and 60b is being fed to switch circuit 68a and 68b and spin cycle control circuit 96 is giving out high signal on line 97 which is an indicative of decision to take weight measurements. Differential amplifiers 73 provide enabling signal for gates 72a and 72b. Differential amplifier 73 only pass an enabling pulse on a positive half cycle of the input signal. When switches 68a and 68b are enabled the positive half or sine force signal passes to weight meter driving circuit 70a and 70b respectively. The weight meter driving circuits integrate input from respective switches and stores the value. A buffering circuit is also employed to retain the last meter reading proving operator enough time to apply the necessary corrective balancing weights to rim 11 and 13. [4]

The encoder and optical switch assembly 14 produce a train of a two-phase displaced pulse as per the shaft rate of rotation. This assembly 14 includes a disc 15 attached to the shaft 10 and has multiple windows 16, as shown in figure 2.1, uniformly spaced from each other along the disc periphery. These windows have width exactly equal to the spacing between two adjacent windows. The assembly 14 includes two

optical switches 18a and 18b mounted on housing 19 which is rigidly attached to the shaft bearing housing 21. Switch housing 19 is U-shaped and surrounds aperture edge of disc 15. Optical switches 18a and 18b includes a light source on one side of disc and phototransistor on the other side. Switches 18a and 18b are spaced with a distance equal to one and one-half of window spacing and they register with the windows, so the signals from 20a and 20b will be out of phase by 90 degree with each other. The direction of phase displacement is dependent on the direction of revolution of shaft 10. [4]

Line 20a and 20b from optical switches directs analog signals to a count pulse producing circuit 78 which, provides either a count-up pulse to 80a or a train count-down pulse to 80b, depending on the direction of rotation of shaft 10. The lines 80a and 80b are connected to first up-down counter 84a and then to second up-down counter 84b. 80a is connected to up-count inputs whereas 80b is connected to down-count inputs. These counters have counting capacity equal to the total number count-up and count-down pulses that are generated in one revolution of a shaft by circuit 78. [4]

The up-down counters 84a and 84b are reset in accordance with respective corrective balancing weight position in planes P1 and P2 as indicated by selected phase angle of the force filter signal 60a and 60b respectively. When the imbalance weight with respective planes P1 and P2 is up, the selected phase angle is zero. As a result of resetting counters at selected zero degrees phase angle that is when the imbalance is at top dead center, the counter output will be at mid-count. Mid count is the count equal to one-half of the counting capacity. When the imbalance weight is at bottom dead center, the corrective balancing weight placement will be at top dead center. [4]

The digital output from counter 84a and 84b are applied to digital-to-analog converter 86a and 86b respectively. These converters provide analog ramp voltage to position meter driving circuit 88a and 88b. Mid-point of voltage ramps are set to

zero degree by D/A circuits. The position meter driving circuit comprises of the differential amplifier unit which causes output voltage from D/A converters to move from maximum negative to maximum positive in a narrow band with mid-point set to zero volts so that the meter 40 and 41 are more sensitive to small increments of shaft rotation. In order to find the location at which the corrective balancing weight is to be placed, the rim is rotated until the position meter 40 or 41 reads zero volts, i.e. null reading. The wheel can be rotated in either direction to get the null reading.

TDC position is used for corrective weight emplacement is only used for operators convenience, as such any emplacement orientation can be used in balancing of wheel using the wheel balancer explained here. With some relatively simple and inexpensive modifications in electronic components, the corrective balancing weight emplacement position can be changed. [4]

The logic circuit for re-initializing up-down counters 84a and 84b in accordance with phase of signal from force filter 60a and 60b comprises of following things, a differential amplifier, a NAND gate, a capacitor. Positive going edge of differential amplifier 73 is connected to NAND gate GI through capacitor C1 as shown in figure 2.2. In order to reset first up-down counter 84a, differential amplifier 73 receives output sine wave signal from filter 60a. Signal from filter 60a has phase related to location of corrective balancing weight in plane P1. Differential amplifier 73 emits a square wave signal with square wave having transition from negative to positive when a sine wave imbalance signal from filter 60a has zero phase angle. The leading edge of square wave which coming from the differential amplifier thus coincides with point in time when the imbalance location in the plane P1 of rim 11 is at the top and the emplacement position for corrective balancing weight on rim 11 is at the bottom. At this point signal from differential amplifier is used in conjunction with signal from spin cycle control circuit 96 through line 97 to enable AND gates 72a and 72b which in turn enables switches 68a and 68b to pass the imbalance force signal from filters

60a and 60b to 70a and 70b respectively. The leading edge of the square wave signal from differential amplifier 73 is passed through capacitor C1 and applied to NAND gate G1 along with signal from line 97. As the output of differential amplifier goes high, NAND gate output goes low which in turn resets the counter 84a. At the end of the testing cycle when the positive signal from line 97 is terminated, no further reset signal can be emitted therefore counter continues the cycle with the starting point for wheel speed based on last reset value received. Switches 68a and 68b will become disabled simultaneously, thereby keeping weight meters 38 and 39 readings fixed. Logic circuit for resetting second up-down counter 84b works in similar manner as explained above for first counter 84a. [4]

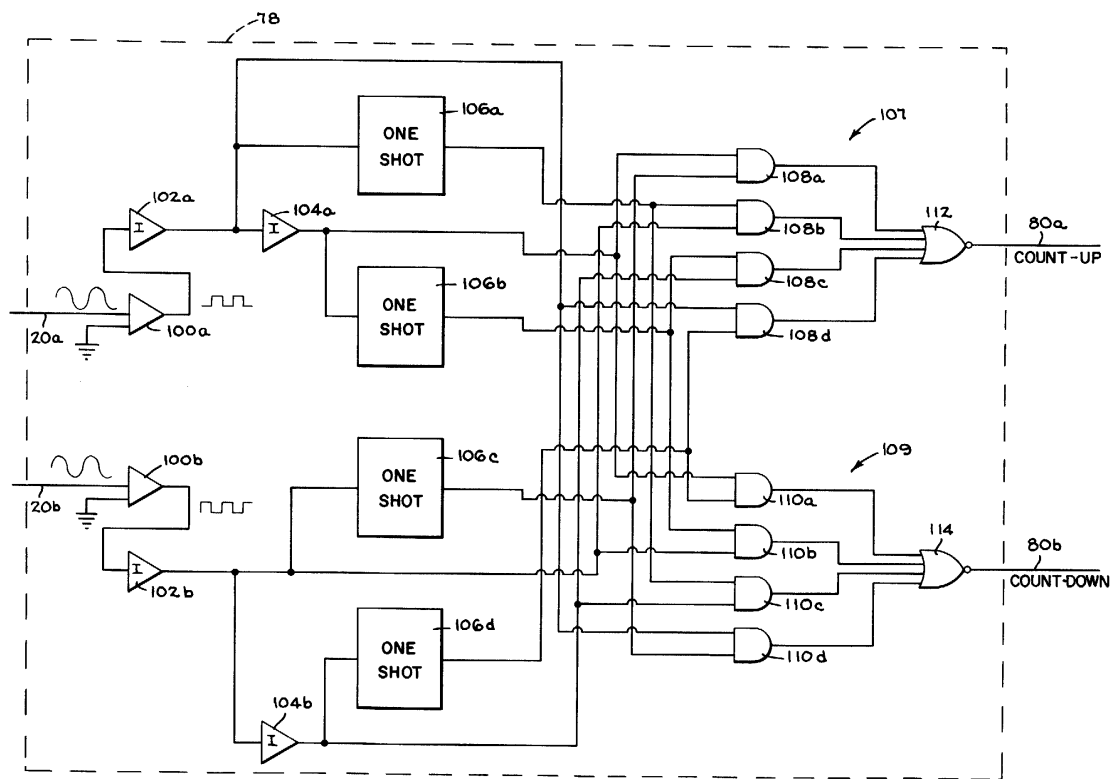


Figure 2.4: Count pulse circuit
[4]

Figure 2.4 illustrates the working of count pulse circuit 78. It comprises of two comparators 100a and 100b which squares the signal on line 20a and 20b respectively.

Due to the phase difference in the signals of two optical switches 18a and 18b, the output from first comparator 100a will lag or advance second comparator 100b by 90 degrees. As indicated in figure 2.2 and 2.3 the shaft is spinning in clockwise direction thus analog signal read by switch 18a will lead signal on switch 18b by 90 degree and hence signal on comparator 100a will signal on comparator 100b by 90 degrees. Output of comparator 100a and 100b are connected to a pair of inverters 102a and 102b respectively. Output from inverters is applied through a logic circuit which consists of two inverters 104a and 104b and four one-shot circuits, to a first AND/OR invert gate 107 consisting of a bank of four AND gates (108a, 108b, 108c and 108d) and one NOR gate 112 and a second similar AND/OR invert gate 109 as shown in figure 2.4. NOR gate (112 or 114) provides count-up pulse when one of the four AND gates produces an output signal. This arrangement of logic circuit works as a pulse multiplier circuit which provides four count-up or count-down pulses for each input pulse from line 20a or 20b. The AND/OR invert gate 107 provides train of output pulses four times the frequency per input pulse on line 20a thereby giving multiplication factor of 4. Accuracy of ± 1.4 can be achieved with 64 equally spaced windows on encoder disc and multiplication factor of 4. [4]

Motor M is spun to rotate wheel W at certain preselected speed. When shaft speed reaches this preselected speed value, the speed detection unit senses this condition and gives signal to reverse power winding of motor thereby shaft 10 comes to a quick stop. When shaft speed detection units sense zero speed, reversing signal to motor is canceled and motor remains in stopped position. It is important that measurements are taken with wheel spinning at general vehicle wheel speed. [4]

Operation of above discussed wheel balancer apparatus: Once wheel W is mounted on wheel balancer shaft operator pushes start switch 44 thus activating motor is forward direction. At the same time, high signal is emitted on line 97 which initiates measurements for balancing weight and location. After reaching the preselected value

of speed, the measurements are taken. At this point control circuit 96 reverses motor power winding to brake the motor thereby stopping the rotation of balancing shaft. At the next instance, the control circuit 96 disables signal on line 97 causing switches 68a and 68b to open, also reset pulses are no longer produced by NAND gates GI. Thus, corrective weight measurements in weight meter 38 and 39 and counter 84a and 84b are retained to the time when stop sequence signal was initiated. When shaft reaches zero speed, motor braking mode signal is removed thereby leaving the apparatus in stopped position. The counters 84a and 84b start counting pulses from the starting position with the imbalance magnitudes as indicated by respective weight meters, such that position meter which is associated with counters indicate null. The corrective weight of the indicated magnitude should be fixed at the top dead center of the respective rim. The operator turns the wheel until one of the position meters is nulled, and places indicated corrective balancing weight at indicated rim location. At any point in time during the balancing operation stop switch 46 can be used to interrupt the operation and stop shaft rotation. [4]

2.3 Wheel Balancing Weight

Newly manufactured tire will have a minor imbalance and it can be corrected by adding corrective balancing weight to a specified location to counter the imbalance effect. Used tires will usually have more imbalance as compared to new tires and it can be compensated for using wheel balancer. If an excessive amount of weight is required to correct the imbalance tire then it may be an indication of the tire being defective or the tire might be incorrectly mounted on the rim. It is possible to have vibrations in balanced tire due to wheel hop. The wheel run-out of less than 0.03" will not induce remarkable vibrations in wheel assembly but for run-out of more than 0.125" it is recommended to replace the tire or wheel. [5]

2.3.1 Type of Wheel Weights

For correcting imbalance in tire/wheel assembly balancing weight suggested by wheel balancer is attached to the wheel rim. The balancing weights to be attached to the rims are being researched on for over 100 years. There are basically two types of wheel balancing weights, clip-on or hammer-on weights which are attached to the rim with the use of wheel weight hammer, and tape-on weights which are stuck to the inside barrel of rim using adhesive.

In early age, before the development of adhesive tape-on weights, clip-on weights were only in use. There are different types of hammer-on weights available in 0.25 ounce of increment. Different types of hammer-on weights are available to conform to various available rim types. Aluminum wheels which accommodate hammer-on weight may need a coated or special alloy clip weight which will not corrode or damage the wheel. These hammer-on lead weights of the various denomination for a different type of rims is knocked onto the edge of the rim with a plastic hammer as shown in figure 2.5. [1]



Figure 2.5: Installation of hammer-on weight
[1]

Wheel rim is analyzed with wheel rim gauge to find out the type of hammer-on weight that can be installed on a particular type of wheel. Rim gauge has multiple profiles marked on it. Rim of the concerned wheel is compared with each profile carved on the rim gauge until the perfect matching profile for the wheel is found. Figure 2.6 shows how different type of hammer-on weight conforms to the particular type of rims. [5]

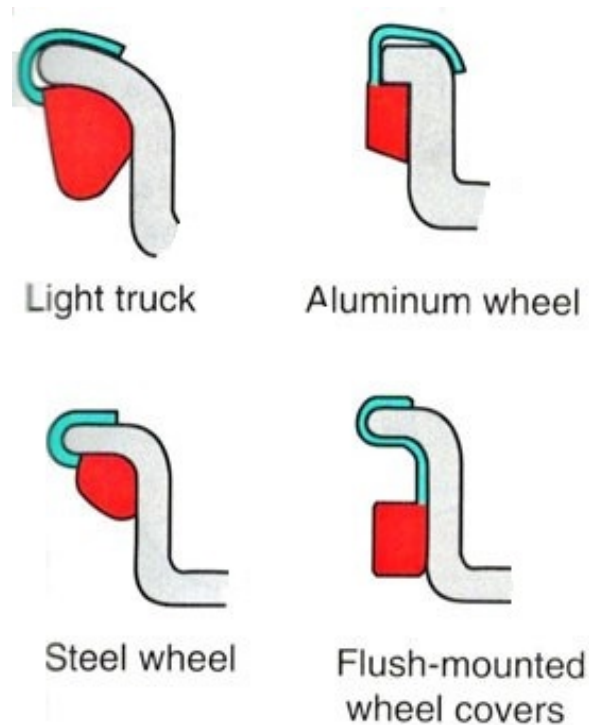


Figure 2.6: Hammer-on weight clip profile [5]

Wheel weight can be of following three material, lead, zinc, or steel. Due to the environmental impact of lead, use of a non-lead material is nowadays promoted. Today, in the USA, many states have passed the legislation which calls for a ban of conventional lead wheel balancing weights. US Environmental Protection Agency (EPA) is actively working on forming new rules that would ban conventional lead weights at the federal level. Legal alternative for lead weights is zinc weights and coated steel weights. Zinc has closest to lead functionality and fit and it is used by most of the

OE manufacturers. It has superior corrosion resistance property and it is softer than steel, thereby reducing the risk of damaging the rim. Steel weights are the popular choice among several North American and few Japanese OE manufacturers. It provides better retention and ensures solid attachment. [6]

Hammer-on weights are the best choice when the rim is of steel. Nowadays most the high-performance vehicles are equipped with alloy wheels. The hammer-on weights tend to break through the coating on expensive painted aluminum when these weights are clipped onto rim's cosmetic face. Thus, water can contact the aluminum beneath the coating causing corrosion. Also, hammer-on weights can be seen from outside and thereby reduce the aesthetic beauty of the wheel. To avoid these problems, tape-on adhesive type weights are often used. [1]

2.3.2 Hammer-on Weights

Hammer-on weight has a weighted body and a clip attached to it. The weighted body has a recess formed in it, and the clip has a securing portion formed to be positioned within the body recess and a grasping portion for holding securely to the exterior rim flange. Such wheel balancing weight has clip secured to it in axial, radial and circumferential direction with reference to the axis of rotation of the wheel and balancing weight body is well-positioned with such wheel. [7]

As explained in research by Shelah Phillips in [8] a pneumatic tire which is mounted on a rim with external flange where hammer-on weights can be clipped is must to make use of hammer-on weights for balancing. Similar research is carried out by Chris C Zang in [9] which is concerned with the type of wheel mentioned above, a wheel with a rim having a flange on which balancing weight can be clipped on. In research by Chris Zang, a modified clip was used for the wheel weight known as half clip. This type of weight has a clip and a weight body as two different units attached to each other by means of a fastener.

Generally, a wheel with tire mounted on it is spun on wheel balancer to calculate

the imbalance and balancing weight as shown in the figure 6 below is clipped on the rim. Rim typically has two locations where a hammer-on weight can be attached, an inside flange and an outside flange. Each flange of a rim defines a circumferential pocket section adjacent to the wheel, balancing weight body should be nestled with this pocket to achieve proper balancing. [7]

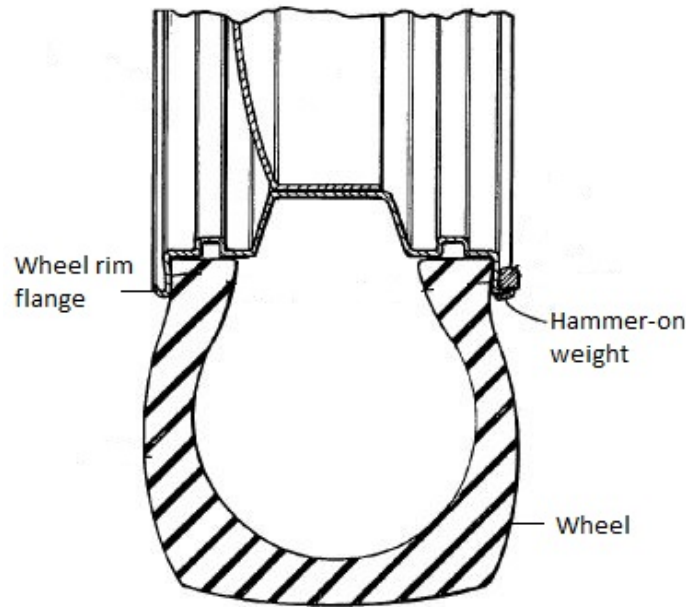


Figure 2.7: Cross section of wheel with hammer-on weight applied
[7]

The clip of the hammer-on weight is constructed in a perfect shape and manner using a durable material such as spring steel as it has to attach weight body securely to the flange. Unlike weight clip, weight body be formed out of any particular material and manner. For environmental reasons, the material used for weight body construction is other than lead. Materials easier to work with processes such as stamping, forming, rolling, pressing are used. For example, steel, copper, brass or zinc.

Earlier when lead was used in construction, wheel balancing weight was formed typically by positioning molten lead around a portion of the clip with an aid of a mold. In the scenario where a material other than lead is used for construction such

as steel, which has a melting point higher than that of lead, a similar technique is not feasible as hot molten steel would tend to melt or deform the clip. In such case weight body and clip are constructed separately and then attached to each other.

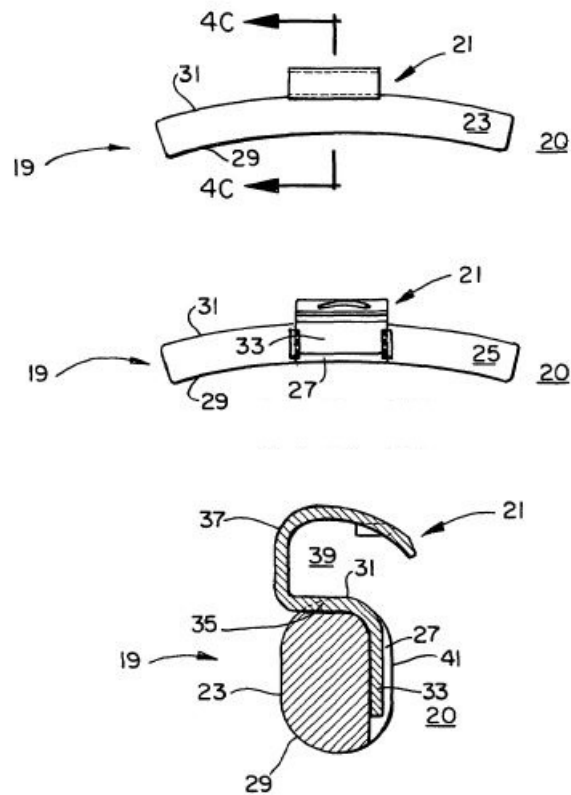


Figure 2.8: Cross section of hammer-on weights
[7]

As shown in the figure 2.8, the weight body generally extends in an arcuate manner so that it can follow the circumferential pocket on the wheel rim near flange. The clip recess is usually centered in position with respect to the arcuate extent of the weight body. Note that it is not necessarily required to have clip recess in the center position for balancing purpose. It is only for the aesthetic purpose that it is placed in the center.[7]

As seen from the figure 2.8 clip 21 of the weight body 20 is formed to have a grasping portion 37 by which clip securely grasp on wheel flange at an appropriate

circumferential location. Grasping portion 37 of the clip co-acts with portion 35 to perform the grasping operation. Axial portion 35 and grasping portion 37 together forms the compartment 39 of the clip 21 within which wheel flange is received.

The clip 21 is fastened to weight body 19 within a recess 27 by use of metal working processes such as crimping, soldering, welding, or fusing. External fasteners such as screws, rivets or external welding is avoided as it will damage the wheel by scratching or scoring on installation or removal of wheel weight on rim flange.[7]

The clip 21 and body 19 of the balancing wheel weight is usually provided with a surface having a high coefficient of friction for effective gripping and to avoid slippage with respect to rim flange. Such surface maybe developed during manufacturing or maybe imparted afterward with an appropriate coating. [7]

It is possible to make further modifications in the hammer-on weight as described above. For example, clip 21 can be fastened to weight body 19 at location other than what is described above and still perform same balancing function. [7]

2.3.3 Tape-on Weights

Hammer-on weights made out of lead were used, conventionally, for balancing wheel. An alternative type of wheel weight types has been researched on for more than 80 years now. In early research done by Skelton and Dreher unitary lead wheel with adhesive to attach on wheel rim is described. These type weights are inconvenient to work with. They are difficult to cut as per the requirement and also difficult to stick on to the rim [10]. As per the research carried out by Kennedy, Skidmore and Griffith it is an old method to apply unitary lead wheel balancing weight to wheel rim by means of an adhesive. Their research explains that it is old to notch a unitary lead weight strip into incremental weight value but it doesn't disclose a plurality of pre-formed integral weight connected in end-to-end relationship upon an elongated adhesive tape which can be separated into predetermined weight values by simply severing the tape. The invention of Hubert D. Songer describes a system of wheel

balancing weight including a single elongated tape long enough to be coiled upon itself which supports on the top surface a plurality of uniform lead weight in end-to-end relation. Each predetermined balancing weight unit weighs 1/4th of an oz. [11]

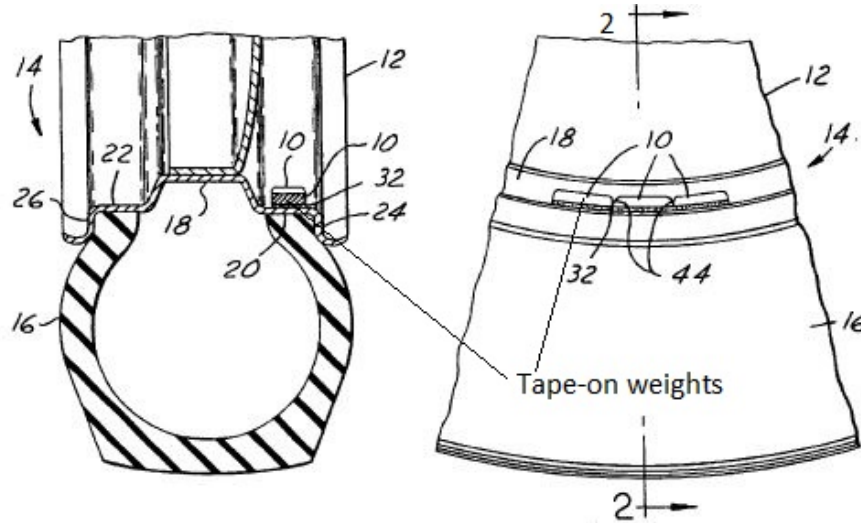


Figure 2.9: Tape-on type wheel balancing weight
[12]

In a recent invention of the wheel balancing weight by Michael M. Pursley stick-on type wheel balancing weight is described having a plurality of uniform wheel balancing weight attached on the top of an elongated adhesive tape. Adhesive tape is provided with a removable backing strip for protecting adhesive layer. Backing strip in this invention has a size larger than the adhesive tape to facilitate the removal of backing strip from adhesive tape prior to installation of wheel weight onto wheel rim. The operator may simply grab onto the backing strip to peel it off since it has a greater width as compared to adhesive tape. A plurality of weights are connected end-to-end and each unit in this series is of uniform size and weight. As per the requirement, any number of plurality of weights may be taken out from the remainder by merely severing the tap, to provide a discrete wheel balancing weight unit. As the required number of balancing weights are removed from the remainder of the weights, the backing tape is removed and the adhesive surface is stuck to inside barrel of the rim at the desired

ily, its size is kept greater than the adhesive tape. Preferably, it is 1/16th of an inch greater than adhesive tape. Stick-on weights are attached to the inside barrel surface of the rim as shown in the figure 2.10. [12]

2.3.4 Curvature Effect of Wheel Balancing Weight

It has been observed that larger the wheel weight, either hammer-on or stick-on, have an effective weight which differs from the actual weight applied to the rim. The effective weight is measured by force transducers. This difference is caused by the curvature of the weights. The wheel weight curvature shifts the center of gravity of some large weights towards the wheel center. For example, if accurately weighed 3 oz. weight is applied to perfectly balanced wheel, the wheel balancing machine will show required balancing weight as 2.92 oz. instead of 3 oz. weight which is applied to the wheel. Moreover, accurately calculated 2.92 oz. wheel weight will not be able to balance this wheel as 2.92 oz. weight will have effective weight approximately equal to 2.82 oz. More the imbalance more is the error. As weight increase, the size of weight also increases and so does its curvature. Also smaller the rim diameter, sever is the curvature effect error. Since with smaller rim diameter, weight curvature increases to conform to the rim shape thereby increasing curvature effect error. This effect can be observed from the images shown below. [13]

The plots shown in the figure 2.11 are formed from the data received experimentally by wheel balancing measurements on aluminum alloy wheel of 14 and 15, with stick-on weight attached to 15 rim at inside diameter of 13.2 and hammer-on weight attached to 14 rim at the rim flange. Since the effective radius of weight location is smaller in case of 15 rim, the curvature effect is more on the wheel of 15 rim. The empirical formulae to calculate curvature effect on 14 and 15 rim are respectively as follows [13]:

$$\textit{Weight - with - curve} = (\textit{stampedsiz}e - 1.25\textit{oz}) * 1.0526 + 1.25\textit{oz}$$

And

$$\textit{Weight - with - curve} = (\textit{stampedsiz}e - 0.5\textit{oz}) * 1.082 + 0.5\textit{oz}$$

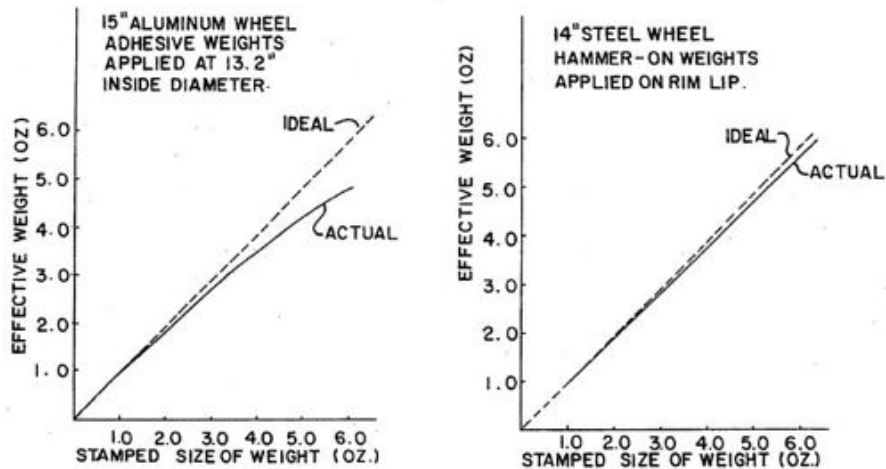


Figure 2.11: Curvature effect of balancing weight
[13]

2.4 Calibration of the Apparatus and Improvement of Imbalance Determination

When the wheel/tire assembly is spun on wheel balancer it gives the measurement of wheel assembly imbalance. In addition to this imbalance, there could possibly be imbalance in wheel balancer spindle itself. The imbalance in wheel balancer spindle affects all the measurements taken by sensors to calculate wheel imbalance. Hence, it is important to compensate spindle imbalance to get accurate wheel balancing measurement. Compensation of wheel balancer spindle and other residual imbalance in machine is carried out by calibration of the wheel balancer. It is important to calibrate every wheel balancer to compensate for various manufacturing components such as wheel balancer spindle, force transducers, electronic circuit involved. [14]

2.4.1 Wheel Balancer Quick Calibration Check

Quick calibration technique as invented by researcher Michael W. Douglas, is used in Hunter latest wheel balancing machines. As per this invention a wheel balancing machine is equipped with quick calibration check which determines if machine is properly calibrated or not. To properly measure imbalance of the wheel, it is important to calibrate the machine since machine's performance might be affected by transducer's

drift' i.e. a transducer producing a response different than what it is calibrated for. Wheel balancer's performance may also get affected by other factors such as machine's age, surrounding temperature, mechanical wear. Improperly calibrated machine will give erroneous measurements about the balancing weight and location. Even after the machine is properly calibrated, the operating conditions can change, thereby requiring machine to be re-calibrated. An accidental occurrence of machine requiring calibration is undesirable as it can lead to significant delays in balancing operation. To avoid this delay, most of the operators check machine for calibration periodically. This is also time consuming. What is more desirable is a quick calibration check method. [15]

Rothamel invented an automatic, self-calibrating wheel balancer machine. Machine described in his invention avoids the need of calibration check regularly. This machine has a secondary shaft with a known imbalance which operates at a different frequency than the primary balancing shaft. Wheel balancer measures the imbalance of the secondary shaft and compare it with known data and thus makes sure that machine is correctly calibrated. Though this invention is useful in self-calibrating the machine, it has drawbacks such as additional cost in manufacturing due to the secondary shaft assembly as well as the secondary shaft induces extra vibration to the machine.[16]

Mitchell invented a similar self-calibrating wheel balancer [17]. He uses four strain gauges to detect imbalance of rotating wheel in his invention. Strain gauge output is passed through a series of analog filters and pre-amps. Mitchell calibrated the filters and pre-amps for every spin by passing a square wave through analog electronics. Output from this circuit is compared to an expected result to determine the calibration, and to decide the correction factor which is to be applied to pre-amps and analog filters. However, this machine does not check for strain gauge drift. If the strain gauge output of this invention is incorrect for any reason it would not be detected by

device calibration system. Hence quick calibration system as described by Michael W. Douglas, is more reliable.[15]

In this invention, the calibration is checked by turning wheel balancer on, mounting calibration weight of known mass to wheel balancer hub at known location, spinning the hub/spindle with this test conditions and then determining imbalance of the test weight/hub assembly. The measured imbalance is compared with predetermined imbalance value and the difference is calculated. If this difference is within the tolerance limit then the wheel balancer is in calibration. Wheel balancer panel displays a result of calibration check indicating whether balancer is calibrated or not.

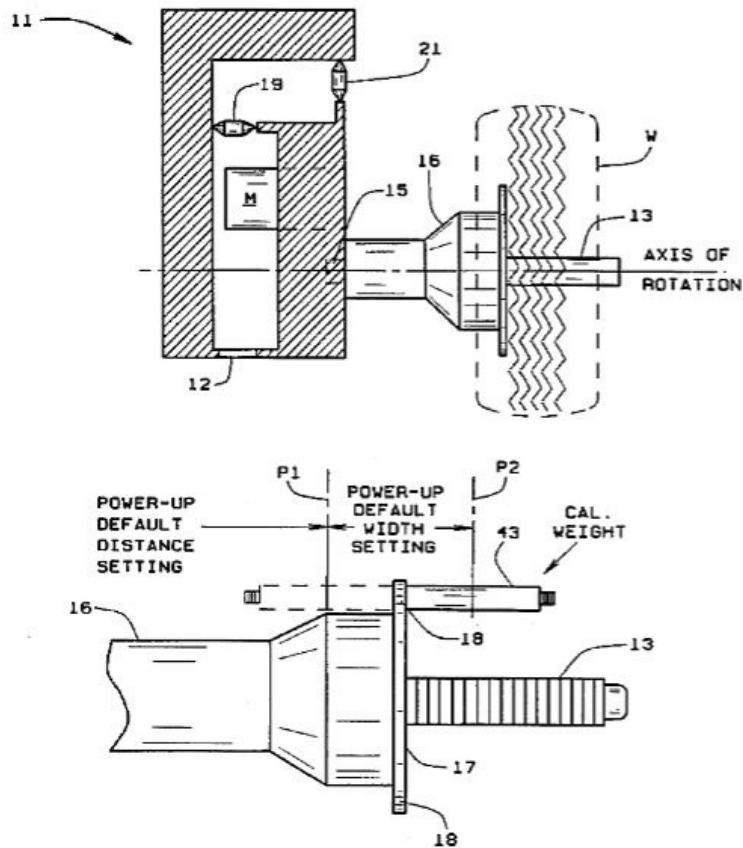


Figure 2.12: Quick calibration mode
[15]

Figure 2.12 shows the simplified view of wheel balancer. It has a rotating shaft 13

driven by motor M. Wheel/tire assembly for balancing test is mounted resting against the spindle hub 16 which is clearly visible in lower part of figure 2.12. Plate 17 is attached to hub 16 with two threaded holes to attach calibration weight placed 180 apart at the same radial distance. As described in the invention mentioned above, wheel balancing unit includes a piezoelectric transducer coupled to balancer spindle to measure the imbalance force. Electronic circuitry for determining imbalance includes anti-aliasing filters, analog-to-digital converter, a digital signal processing (DSP) chip, a motor controller, a display, and an input device. An electronic control arm connected to DSP chip having a position sensor is used to give input to wheel weight plane location.[18]

Default setting for the calibration check defines two calibration planes P1 and P2 respectively as shown in lower part of figure 2.12. These planes coincides with the center of gravity of calibration weight when attached on left or right side of the plate 17. Test weight 43 which is an elongated cylinder of known mass is mounted on plate 17 at a known predetermined location to check for calibration. This calibration test weight has a threaded end which is screwed to one of the holes numbered 18 in lower part of figure 2.12 on the plate 17. Test weight can be mounted on either side of the plate 17. In fig 2 weight is shown screwed to outer side of the balancer i.e in plane P2. As described in the Fig. 5 below, after the wheel balancer is turned on, DSP unit, uses the default wheel parameter for plane P1 and P2 and spins the balancer spindle with test weight 43 and performs balancing operation to determine imbalance of hub/test weight assembly. [15]

As the test weight is of predetermined know mass and location, and DSP unit is updated with the test weight parameter, the imbalance calculated by machine for test weight should be equal to predetermined value if the machine is well calibrated. DSP chip compares the imbalance measured with the expected value and if the difference, if any, is within the set tolerance, for most cases it is 0.05 oz., DSP generates CALRDY

message on the display indicating that machine is calibrated and can be used for balancing purpose. [15]

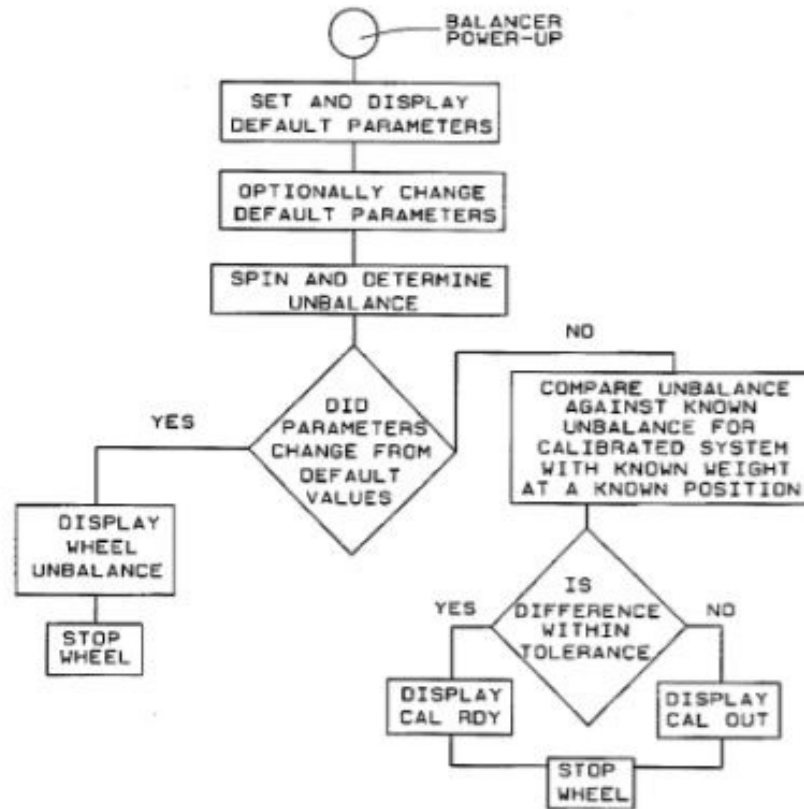


Figure 2.13: Flowchart for calibration check
[15]

If difference is not within the tolerance, the DSP displays CALOUT message on the display panel. A broader tolerance can be used in order to accommodate for changing environmental conditions such as temperature. Wheel balancer in this invention, thus provides a simpler way to check for calibration by display CALRDY, CALOUT messages. Instead of relying on CALRDY, CALOUT messages as displayed by DSP, Operator can measure imbalance magnitude and position and himself determine if it is within the tolerance or not by comparing to the standard values. It is, however, preferable and convenient that DSP makes this determination. [15]

Whenever the balancer is turned on and put into calibration check mode, a flag

in turned on. If the operator uses dataset arm to change the predetermined input, the flag is turned off. The balancer checks this flag and decides whether to run a calibration check or imbalance measurement. After the calibration check is performed, the balancer turns this flag off. [15]

CHAPTER 3: MATHEMATICAL EQUATION OF WHEEL BALANCING OPERATION

3.1 Mathematical Equation of Wheel Balancing

Wheel balancer is equipped with force transducers, to measure imbalance forces acting spindle shaft and encoder, to find out the angular location of imbalance forces. There are many different combination possible for placement of force transducer and encoder. For this study lets consider the combination as explained in chapter 2, section 2.2. Figure 3.1 shows the top view of wheel balancer shaft. It consists of encoder on the leftmost end. Two force transducer F_1 and F_2 in horizontal plane as shown in the figure. Distance between two force transducer is a . Wheel is mounted on spindle shaft and tightened with wingnut on the rightmost end of shaft. P_1 and P_2 are two weight location planes on wheel. Distance between P_1 and P_2 , or wheel width, is c . Distance between inner weight plane P_1 and force transducer 1 is b .

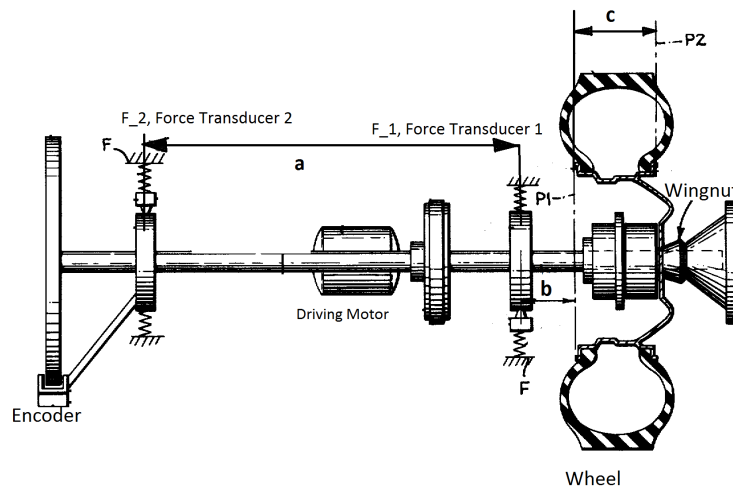


Figure 3.1: Force transducer and encoder assembly on spindle shaft

Force transducer measures forces acting at the force transducer location on spindle shaft. Encoder records the angle when forces in weight planes P_1 and P_2 are optimized. Force transducers and encoder transmits signals to digital signal processor (DSP). The working of these sensors and DSP for balancing calculation is explained in details in chapter 2, section 2.2. In this chapter only mathematical equations involved in wheel imbalance force calculations are discussed.

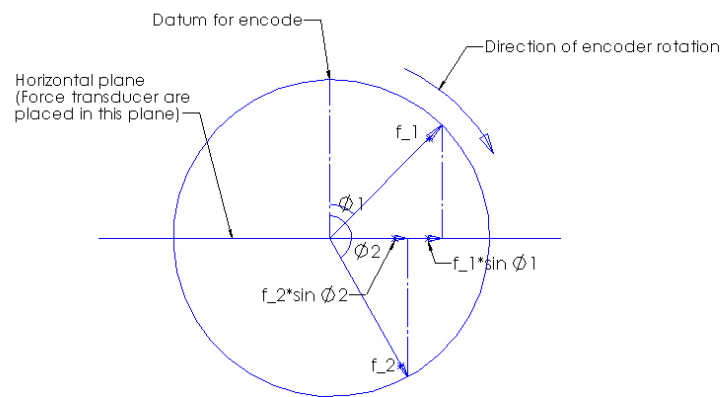


Figure 3.2: Imbalance forces in wheel plane
[4]

Figure 3.2 shows the imbalance forces f_1 and f_1 acting in wheel plane P_1 and P_2 respectively. Encoder records the angular location when these forces are optimized and stores the value. ϕ_1 and ϕ_2 are the angular measurements of the forces f_1 and f_1 from encoder datum as show in the figure 3.2. Forces generated by imbalance mass are centrifugal forces and hence as shown in figure above, they are acting outwards. Since force transducers are installed in the horizontal plane, we need to find out the horizontal component of forces f_1 and f_1 to deduce force balance equations. The horizontal components of these forces are $f_1 \sin \phi_1$ and $f_2 \sin \phi_2$.

Figure 3.3 is the free body diagram of force acting on spindle shaft of wheel balancer shown in figure 3.1. Forces measured by two force transducers are denoted by F_1 and

F_2 . Direction of these forces in towards centerline of spindle shaft as shown in the figure.

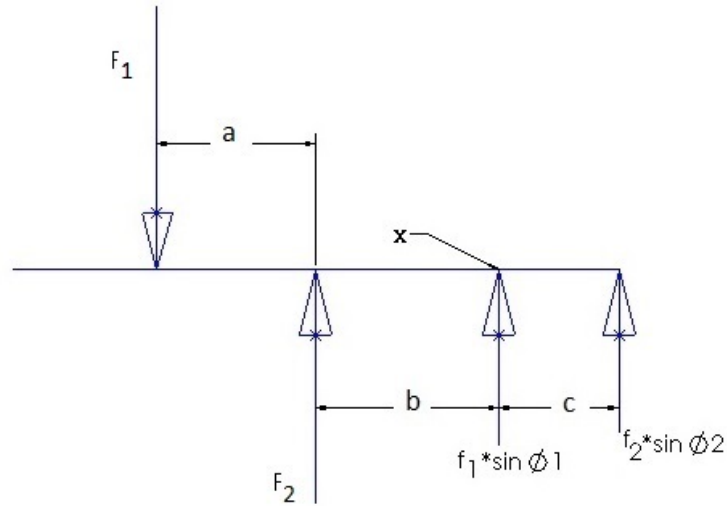


Figure 3.3: Force transducer and encoder assembly on spindle shaft [4]

Lets write down the equation of force balance on spindle shaft:

$$\sum F = 0 \quad (3.1)$$

$$\therefore -F_1 + F_2 + f_1 \sin \phi_1 + f_2 \sin \phi_2 = 0 \quad (3.2)$$

$$\therefore f_1 \sin \phi_1 = F_1 - F_2 - f_2 \sin \phi_2 \quad (3.3)$$

Writing down the moment balance equation at x ,

Considering clockwise moment to be positive.

$$\therefore f_2 \sin \phi_2 * c + F_2 * b - F_1 * (a + b) = 0 \quad (3.4)$$

$$\therefore f_2 \sin \phi_2 = F_1 * a/c + b/c * (F_1 - F_2) \quad (3.5)$$

In the above equations value of forces F_1 and F_2 are received from force transducers and angular position values ϕ_1 and ϕ_2 are received from encoder. Forces acting in the weight planes P_1 and P_2 are calculated from equations above.

$$f_1 = [F_1 - F_2 - F_1 * a/c - b/c * (F_1 - F_2)] / \sin \phi_1 \quad (3.6)$$

$$f_2 = [F_1 * a/c + b/c * (F_1 - F_2)] / \sin \phi_2 \quad (3.7)$$

Equations 3.6 and 3.7 states the value of forces acting in weight planes ϕ_1 and ϕ_2 respectively.

If weights used to balance the wheel are both hammer-ons, then the locations to attach the weights are at the wheel rim flanges. In that case radial distance of both the weights will be equal. In case of combination one hammer-on and one stick-on weight, the radial distance of both the weights will be different. Let r_1 and r_2 be the radius of weights in plane P_1 and P_2 . Let ω be the angular velocity of the wheel balancer shaft.

The masses to attach in two weight planes to balance the wheel are as follows:

$$\begin{aligned} m_1 &= f_1 / (\omega^2 * r_1) \\ &= (F_1 - F_2 - F_1 * a/c - b/c * (F_1 - F_2)) / (\sin \phi_1 * \omega^2 * r_1) \end{aligned} \quad (3.8)$$

$$\begin{aligned}
m_2 &= f_2/(\omega^2 * r_2) \\
&= (F_1 * a/c + b/c * (F_1 - F_2))/(\sin \phi_2 * \omega^2 * r_2)
\end{aligned}
\tag{3.9}$$

3.2 Error Analysis of Wheel Balancing Equations

The output of wheel balancing machine or knowledge of any physical system is obtain by taking measurements or doing experiments. Understanding how to express and analyze such data to draw meaningful conclusion from it is important. Measurements of all the physical quantities are subjected to some uncertainties. Error is inevitable but it is important to make error as small as possible. Error should be analyzed and dealt with properly in order to draw a valid conclusion. [22]

Equations 3.8 and 3.9 gives the value of masses required for balancing. These equations depends on following quantities: F_1 , F_2 , ϕ_1 , ϕ_2 , b , c , r_1 and r_2 . 'a' is the distance between two transducer which is constant, hence it is not considered as a dependent variable in this analysis. In this section error analysis of wheel balancing equation is done with respect to above mentioned dependent variables.

For error analysis, if Z is a function of two independent variable A and B with individual errors ΔA and ΔB respectively, then error in Z is related to errors in A and B with following equation ,

Function Z is defined as, $Z = F(A, B)$

Error in Z with respect to independent variable A and B is defined as,

$\Delta Z = (\delta F/\delta A)*\Delta A$ and $\Delta Z = (\delta F/\delta B)*\Delta B$ respectively. [22]

Lets do error analysis of equations 3.8 and 3.9 with respect to F_1 , F_2 , ϕ_1 , ϕ_2 , b , c , r_1 and r_2

Considering the particular case when $\phi_1 = 45^\circ$ and $\phi_2 = 135^\circ$. Considering values of $a = 0.4$ m , $b = 0.2$ m and $c = 0.2$ m. Let correction weight on inner and outer

plan be 1.0 Oz. Putting these values in equations 3.8 and 3.9 to find the values of F_1 and F_2 . The values of F_1 and F_2 as found by reverse engineering method are $F_1 = -0.7545\text{N}$ and $F_2 = -3.7745\text{N}$. Angular velocity of wheel balancer shaft is 15.7 rad/s [20]. Let values of radius $r_1 = r_2 = 17 \text{ in} = 0.4318 \text{ m}$.

Errors in measurement of force and angular location i.e. F_1, F_2, ϕ_1, ϕ_2 are as follows [20]:

$$\Delta F_1 = \Delta F_2 = 0.1 \text{ Oz}, \Delta \phi_1 = \Delta \phi_2 = 0.7^\circ$$

Error induced due to operator in measurements of b, c, r_1 and r_2 is 10 mm or 0.01m as found during the tests.

Using the above values error analysis of mass equations is performed.

3.2.1 Error Analysis of m_1

$$m_1 = (F_1 - F_2 - F_1 * a/c - b/c * (F_1 - F_2)) / (\sin \phi_1 * \omega^2 * r_1) \quad (3.10)$$

1] Relation of Δm_1 with error in F_1 :

To find dependency of error in equation 3.10 with respect to dependent variable F_1 , partially differentiating right hand side of equation 3.10 with respect to F_1 ,

$$\therefore \Delta m_1 = ((1 - a/c - b/c) / (\sin \phi_1 * \omega^2 * r_1)) * \Delta F_1 = 0.00046\text{kg} \quad (3.11)$$

2] Relation of Δm_1 with error in F_2 :

To find dependency of error in equation 3.10 with respect to dependent variable F_2 , partially differentiating right hand side of equation 3.10 with respect to F_2 ,

$$\therefore \Delta m_1 = ((-1 + b/c) / (\sin \phi_1 * \omega^2 * r_1)) * \Delta F_2 = 0.0000923\text{kg} \quad (3.12)$$

3] Relation of Δm_1 with error in ϕ_1 :

partially differentiating right hand side of the equation 3.10 with respect to ϕ_1 ,

$$\begin{aligned} \therefore \Delta m_1 &= (-(F_1 - F_2 - F_1 * a/c - F_1 * b/c + F_2 * b/c) * \cos \phi_1 / (\omega^2 * r_1 * \sin^2 \phi_1)) * \Delta \phi_1 \\ &= 0.000000132kg \end{aligned} \quad (3.13)$$

4] Relation of Δm_1 with error in b :

partially differentiating right hand side of equation 3.10 with respect to b ,

$$\therefore \Delta m_1 = ((-F_1/c + F_2/c) / (\sin \phi_1 * \omega^2 * r_1)) * \Delta b = 0.0021kg \quad (3.14)$$

5] Relation of Δm_1 with error in c :

partially differentiating right hand side of equation 3.10 with respect to c ,

$$\therefore \Delta m_1 = ((F_1 * a + F_1 * b - F_2 * b) / (c^2 * \sin \phi_1 * \omega^2 * r_1)) * \Delta c = 0.0021kg \quad (3.15)$$

6] Relation of Δm_1 with error in r_1

To find relation of error in equation 3.10 with respect to dependent variable r_1 , partially differentiating right hand side of equation 3.10 with respect to r_1 ,

$$\begin{aligned} \therefore \Delta m_1 &= (-(F_1 - F_2 - F_1 * a/c - F_1 * b/c + F_2 * b/c) / (\sin \phi_1 * \omega^2 * r_1^2)) * \Delta r_1 \\ &= 0.0000031kg \end{aligned} \quad (3.16)$$

Total error induced in calculation of m_1 is root of sum of squares of above individual errors. Therefore total error is,

$$\Delta m_1 = 0.00287kg = 0.1012Oz \quad (3.17)$$

3.2.2 Error Analysis of m_2

$$m_2 = (F_1 * a/c + b/c * (F_1 - F_2))/(\sin \phi_2 * \omega^2 * r_2) \quad (3.18)$$

1] Relation of Δm_2 with error in F_1 :

To find dependency of error in equation 3.18 with respect to dependent variable F_1 , partially differentiating right hand side of equation 3.18 with respect to F_1 ,

$$\therefore \Delta m_2 = ((a + b)/(c * \sin \phi_2 * \omega^2 * r_2)) * \Delta F_1 = 0.000554kg \quad (3.19)$$

2] Relation of Δm_2 with error in F_2 :

To find dependency of error in equation 3.10 with respect to dependent variable F_2 , partially differentiating right hand side of equation 3.18 with respect to F_2 ,

$$\therefore \Delta m_2 = (-(b/c)/(\sin \phi_2 * \omega^2 * r_2)) * \Delta F_2 = -0.000185kg \quad (3.20)$$

3] Relation of Δm_1 with error in ϕ_2 :

partially differentiating right hand side of equation 3.18 with respect to ϕ_2 ,

$$\begin{aligned} \therefore \Delta m_2 &= (-\cos \phi_2 * (F_1 * a/c + b/c * (F_1 - F_2)) / (\sin^2 \phi_2 * \omega^2 * r_2)) * \Delta \phi_2 \\ &= 0.000123kg \end{aligned} \quad (3.21)$$

4] Relation of Δm_2 with error in b :

partially differentiating right hand side of equation 3.10 with respect to b ,

$$\therefore \Delta m_1 = ((F_1 - F_2) / (c * \sin \phi_2 * \omega^2 * r_1)) * \Delta b = 0.02kg \quad (3.22)$$

5] Relation of Δm_2 with error in c :

partially differentiating right hand side of equation 3.10 with respect to c ,

$$\therefore \Delta m_1 = ((F_1 * a + (F_1 - F_2) * b) / (\sin \phi_2 * \omega^2 * r_1)) * \Delta \phi_2 = 0.000024kg \quad (3.23)$$

6] Relation of Δm_2 with error in r_2

To find relation of error in equation 3.18 with respect to dependent variable r_2 , partially differentiating right hand side of equation 3.18 with respect to r_2 ,

$$\therefore \Delta m_2 = (-(F_1 * a/c + b/c * (F_1 - F_2)) / (\sin \phi_2 * \omega^2 * r_2^2)) * \Delta r_2 = -0.000465kg \quad (3.24)$$

Total error induced in calculation of m_2 is square root of sum of squares of above individual errors. Therefore total error is,

$$\Delta m_2 = 0.002kg = 0.0705Oz \quad (3.25)$$

CHAPTER 4: METHODOLOGY

4.1 Test Wheels and Wheel Conditions

This research aims to study influence of operational variables on wheel balancing measurement. With the introduction of some super low profile tires, some general areas of knowledge and common rules of thumb are becoming incorrect extrapolations. The tires used in this study are of modern design with low profile section. The section profile of the tire is the ratio of height of the tire's sidewall to its width multiplied by 100. Just for reference, the second number in a tire designation is profile so a P225/70R16 has a 70% profile. The tire height is 70% of the 225mm width or 158mm. Sections profiles of the test wheels used in this research varies from 35 to 50. The width of the test wheels used in this research varies from 205mm to 265mm. Most of the measurements were taken on Porsche high performance tires. Porsche new as well as old tire design was considered. One set of Porsche tires, old design, were seriously Autocrossed, hence were in worned-out condition and another set of Porsche new design, high-performance tires were only street used, hence were in good condition. These wide range of test tires gave me confidence on my finding and provided me with more precise results. A special hub to mount Porsche high-performance tires on wheel balancer was designed and manufactured which proved to improve precision and repeatability of the measurements. Hub design is discussed in more details later in this chapter.

Designation of the tires used in this research are listed in the table below:

Table 4.1: Designation of the test wheels

Designation	Parent car	Note
205/50 ZR 17 89Y	Porsche 911 Cabriolet	Old design
265/35 ZR 18	Porsche 911 Cabriolet	New design
225/40 ZR 18	Porsche 911 Cabriolet	New design
265/35 ZR 18 (97Y)	Porsche 911 Cabriolet	New design
205/40 R 17 84H	Mazda 3	-
255/40 ZR 17 94(H)	Porsche 911 Cabriolet	Old design

Explanation of the designation used in the table above. For reference consider designation for Porsche old design front tire with designation 205/50 ZR 89Y. In this designation 205 is the tire width in millimeters. 50 is the section profile i.e. the height of the sidewall is 50% of its width. Therefore height of sidewall in this case is equal to $205 \times 0.5 = 102.5\text{mm}$. 'ZR' is the speed rating. Tire with speed rating ZR can run at speed in excess of 150 mph. Tire with speed rating R can run at speed up to 106 mph. 89 in the designation is the load rating, indication of how much load particular tire can bear. Tire with the load rating 89 can bear load of 1297 pounds.

As it can be understood from the explanation above that Porsche tires have high-speed ZR rating. Similarly, most of the high-performance cars use high-speed rating (ZR,W,Y) tires. Imagine the effect of imbalance weight, considering even tiny amount of imbalance, on the tire of a car which is running at 186 mph (300 kmph). Considering the impact of imbalance on high-performance tires, for the measure part of this research tires used for wheel balancing measurements are high-performance Porsche tires. Tire pneumatic pressure was always set to 35 psi during the measurements to eliminate influence of pressure if any, except for the test when the effect of pressure on wheel balancing was analyzed.

4.2 Introduction to Hunter DSP9200 Wheel Balancer

Wheel balancing, also known as tire balancing, is the process of equalizing the weight of the combined tire and wheel assembly so that it spins smoothly on a road going vehicle at high speed. Balancing involves putting the wheel/tire assembly on a balancer, which centers the wheel and spins it to determine where the weights should go. Wheel balancing reduces the operational vibration of wheel assembly of vehicle by calculating the weight of correcting balance weight to be placed on the wheel rim and also its angular orientation on the rim.

Hunter DSP9200 wheel balancing machine is used for this research. One input to the balancing machine is the radial and lateral location of the balance weights, e.g. the wheel rim flange. On the DSP9200, two movable dataset arms are used to input lateral and radial weight location to the digital signal processor. A foot pedal is pressed while positioning an extensible dataset arm that is positioned at the correct radial and lateral position. Figure 4.1 displays the experimental setup for taking wheel balancing measurements



Figure 4.1: Wheel balancer DSP9200 with pointing laser

The specification of DSP9200 wheel balancer are given in the table 4.2:

Table 4.2: Hunter DSP9200 wheel balancer specifications

Power Requirements	196-256V, 3Amps, 50/60 Hz, 1 Ph
Air supply requirement	N/A
Capacity	
Rim width	1.5" to 20" (38 mm to 508 mm)
Rim diameter	10" to 24.5" (254 mm to 622 mm)
Inner dataset range	10" to 28" (254 mm to 711 mm)
Max. tire width	20" (508 mm)
Max. tire diameter	38" (965 mm)
Max. tire weight	150 lbs (68 kgs)
Imbalancer resolution	+/- 0.05oz (1.0 g)
Placement accuracy	512 positions, +/- 0.35°
Balancing speed	150 rpm
Motor	Programmable drive system and DC motor
Machine's weight	475 lbs (215 kgs)

[19]

The figure 4.2 displays various important component of wheel balancer DSP9200. The spindle lock or foot pedal is used to lock the spindle shaft as well as to take the input when dataset arms are put to desired position. Balancing weight location is set using inner and outer dataset arms. The digital signal processing (DSP) unit of wheel balancer commands balancer spindle shift onto which wheel/tire assembly is mounted to spin (when safety hood is lowered) and measures the forces and moments acting on the shaft due to imbalance in the wheel/tire assembly. From these force measurements and knowing the position of the balancing weights placement, it calculates the amount of weight and angular position. The weights are typically of two styles, a hammer on weight and a stick on weight. Type of balancing weight is selected using control on control panel. A common arrangement for modern alloy wheels is to use hammer on weights at the inner flange and then tape on weights near the outer wheel face but hidden behind the wheel spokes. All of the wheels tested in this research were of this

compound weight configuration.

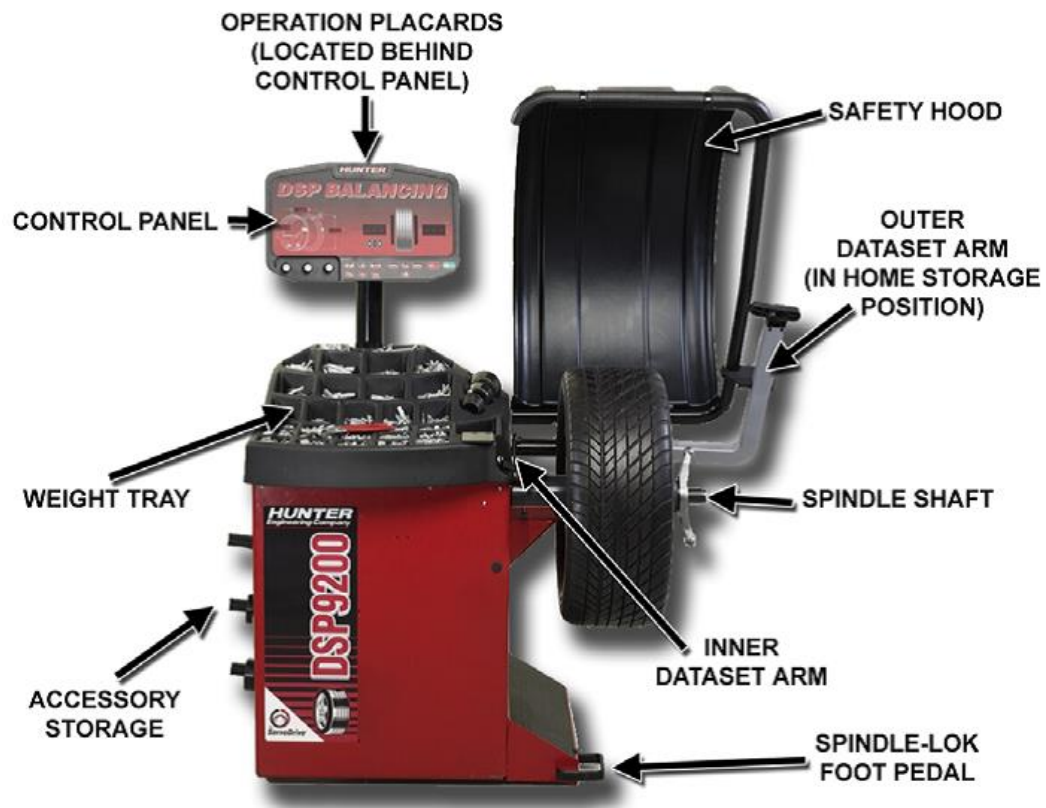


Figure 4.2: Components of wheel balancer DSP9200
[20]

4.2.1 Balancing Overview

Hunter DSP9200 wheel balancer has two balancing modes:

1] Static balance:

In static balancing, the tire is balanced when at rest. For instance, if tire/wheel assembly is placed horizontally on a cone at center and was balanced, then it would be statically balanced.[20]

In static imbalance there is one amount of unbalanced weight located in the center plane of the tire/wheel assembly as shown in figure 4.3, causing an imbalance. As the wheel rotates, this unbalanced weight generates centrifugal force acting in the center plane, causing the tire/wheel assembly to move "up and down" creating bounce in the assembly. In general practice, static balance alone is seldom recommended. The wheel

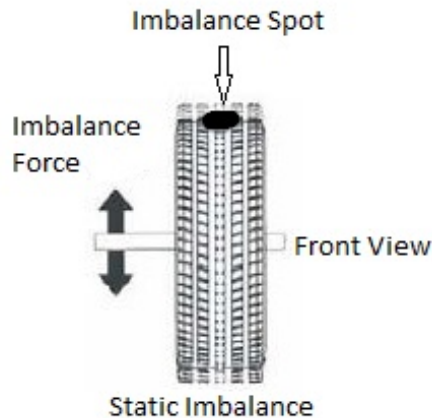


Figure 4.3: Static imbalance
[20]

assembly is usually balanced for static and more importantly dynamic balance.[20]

2] Dynamic balance:

In dynamic imbalance, one or more unbalance heavy weight spots are located in non-centered plane causing an imbalance couple force or imbalance wobble. As shown in figure 4.4 two imbalance spot are 180° radially apart and are on opposite sides. There is also one static imbalance spot as show in the figure 4.4 in the center plane of the wheel. Dynamic balancing function of Hunter DSP9200 directs the operator to place corrective weights on inner and outer correction location of the rim such that static imbalance (imbalance force) as well as dynamic imbalance (imbalance couple/wobble) will be eliminated.

Zero dynamic imbalance = zero static imbalance (up & down) + zero couple imbalance (wobble).

3] Static and Dynamic imbalance sensitivity[20]:

To achieve the best balance, as a general rule of thumb, residual static imbalance should not be more than 1/2 oz. and residual dynamic imbalance should not be more than 1/4 oz. Small amount of residual dynamic imbalance can be tolerated as does not

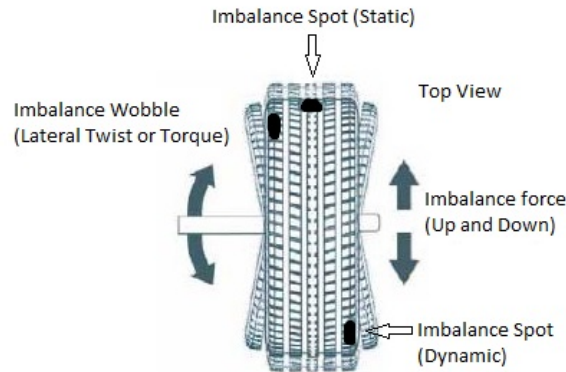


Figure 4.4: Dynamic imbalance
[20]

generate much vibration as compared to small amount of residual static imbalance.

4] Balancing weight planes:

For static balancing using "Standard Balance" mode using hammer-on weights, the input plane is the plane of rim flange on both the sides. As the static imbalance is only in center plane hence to balance it, it is recommended that equal amount of correction weight is placed on each side of tire to reduce the residual dynamic imbalance. While using "Mixed Weight Balance" and "Adhesive Weigh Balance" in static balancing it is recommended that, adhesive type weight is sticked to rim inner barrel as close to centerline of wheel as possible to reduce the residual dynamic imbalance. When using "Patch Balance" mode, patch weight is recommended to place as close to center of the tread as possible. It must be understood from the explanation above that the radial distance of Patch Balance mode weight is highest and that of Adhesive Balance mode is lowest for the same tire.

In dynamic balancing, balancer must know the location of two correction weight placement circles. Placement location is set as input using dataset arms. Figure 4.5 describes the various planes for weight placement defined by various weight mode functions of wheel balancer.

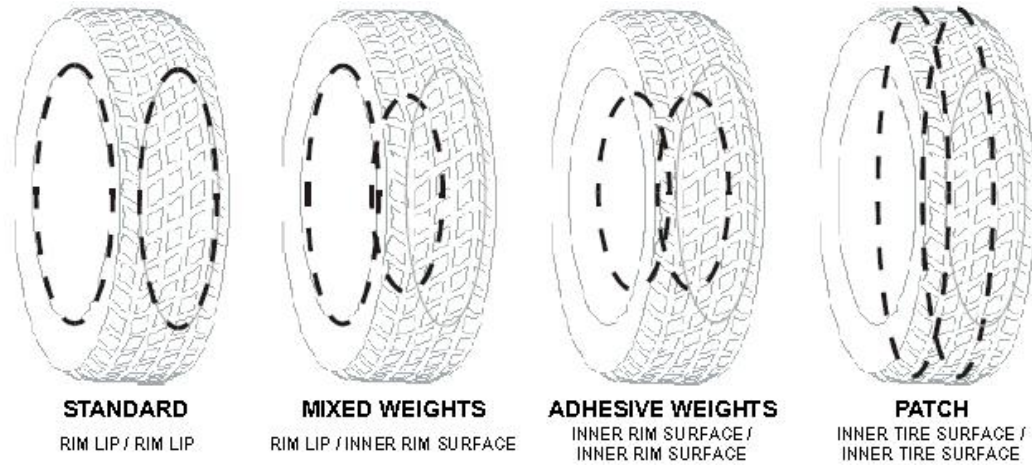


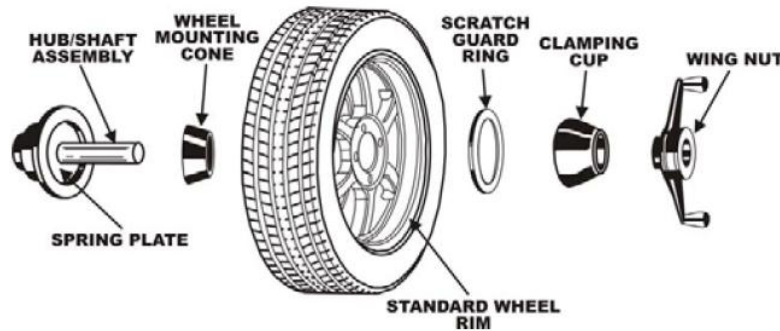
Figure 4.5: Dynamic balance weight planes
[20]

In "Standard Balance" mode one correction weight is applied on each rim flange. In "Mixed weight" mode, one weight is applied on inner flange and one weight is applied to inner rim barrel. Most of the test wheels in this research are balanced using Mixed Balance mode. "Adhesive Weight" mode and "Patch Weight" mode makes use of two planes in inner rim barrel and inner tire tread surface respectively to attach correction weights as shown in figure 4.5.

4.2.2 Balancing Wheel on DSP9200 and Various Features of The Machine

1] Mounting wheel on the wheel balancer spindle: [20]

First step in wheel balancing with DSP9200, or any wheel balancer for that matter, is to mount the the tire/wheel assembly on the balancer spindle shaft. Any unwanted pre-existing weights should be removed before mounting wheel on the shaft. Wheel balancing accuracy depends on the accurate centering of the wheel on spindle shaft hence proper mounting cone should be used for mounting. Hunter DSP9200 is equipped with *CenteringCheck* feature. Once wheel is mounted on wheel balancer using proper mounting cone and tightened against the captivating spring, this *CenteringCheck* feature is used to check if wheel is centered properly on the spindle shaft. DSP9200 is also equipped with *Spindle-Lok* foot pedal, depressing and holding onto



[20]

Figure 4.6: Wheel mounting assembly

this pedal locks the spindle shaft. Holding spindle shaft locked during tightening the wing nut against the wheel, improves the accuracy of centering the wheel on the shaft. There are various combinations of attachments possible for mounting wheel on DSP9200 spindle shaft. The combination used for most the measurement during this research is as shown in the figure 4.6

2] Measuring the wheel dimensions: [20]

Hunter DSP9200 is equipped with Auto Dataset arm which allows to take more accurate and faster rim measurements. Once the wheel is mounted on the spindle shaft, one of the two dataset arms can be used to input the rim distance, rim width, weight plane location automatically, thereby eliminating errors induced due to manual input of dimensions. The dataset arms are positioned in weight plane and the dimensions are entered by depressing the Spindle-Lok foot pedal.

Measuring dimensions on Hammer-on weights: Hammer-on are installed on outside flange of wheel rim. There will be weight on either side of the wheel, when both the weights used for balancing are hammer-on type. To input location of weight plane on the left, inner dataset arm is pulled away from its position to trigger a new left plane reading. Outer dataset arm is pulled towards right plane of the wheel to trigger the location of right weight plane.

Measuring dimensions for mixed and two adhesive type weight: Adhesive type weights are stuck to the inner barrel of the wheel rim, hence both the weights in

this case can be measured using inner dataset arm on the left side as they are only accessible by inner dataset. Inner dataset arm is pulled toward the first from the left weight plane location and foot pedal is depressed to enter the input. The inner dataset arm is then moved to the second weight plane and its location is entered in same way.

Wheel dimensions can also be entered manually using the knobs on the control panel. Auto Dataset arms are more accurate than manual input and for most of this research mixed-weight setting is used and input is provided by inner dataset arm.

3] Standard balancing procedure: [20]

Standard balancing procedure involves following steps. First, wheel is mounted on the shaft. Second, type of balancing is selected using "Static/Dynamic" button. Third, weight type, hammer-on, stick-on or mixed, is selected using "Standard/ALU" button on the control panel. Fourth, depending on the type of weight, inner or outer or both dataset arms are used to take the wheel weight plane location input. Fifth, to initiate the measurements the safety hood is lowered. Once the safety hood is lowered, wheel starts spinning and force transducer takes the force measurements. Location of the imbalance is measured by encoders attached to the shaft. Lastly, once wheel stops spinning, the safety hood can be raised and the correction weight and its location will be displayed on the control panel screen.

4] Other useful features: [20]

There are many useful features of Hunter DSP9200, which makes wheel balancing easy and more accurate. A few of these features are used during this research. **Quick-Thread** feature is an DC drive motor control which helps operator in fast installation and removal of DSP9200 wing nut by making use of DC motor assisted threading. **Spindle-Lok** feature as explained before, locks the spindle shaft of balancer when foot pedal is depressed. Locking the balancer spindle shaft helps in stabilizing the wheel and attaching weights accurately. It also helps in loosening and tightening the wing

nut. **Hood Close Autostart** feature spins the spindle shaft and starts balancing process automatically when the safety hood is closed. After every balancing spin, the safety hood must be lifted up completely before the balancer autostarts again. This feature can be enabled or disabled in the balancer setup procedure. **Loose Hub Deterct** feature can identify if the wheel slips on the spindle shaft, and the balancer automatically stops the operation and displays "LOOSE" on the control panel. Excessively large amount of weights can be split into two smaller weights of equivalent effect by using **Split Weight** feature of the machine. Other features of the machine are not used during this research and hence are not being discussed here.

4.3 Centering of Wheel on Wheel Balancer

Accuracy of the wheel balancing measurement depends on how accurately the wheel is centered on the wheel balancer's spindle shaft. Wheel balancing machine determines the imbalance in wheel/tire assembly by analyzing mechanical vibrations caused by rotating wheel. The imbalance in wheel/tire assembly may result from imbalance in wheel, imbalance in tire, or both. Cause of wheel/tire assembly vibration may not always be wheel imbalance. Even a perfectly balanced wheel can cause significant vibration forces if there is non-uniformity in tire construction or run-out in the wheel rim. Tire manufacturers inspect their tires after construction on tire uniformity machines to reduce constructional errors.

Even when when/tire assembly is manufactured to the utmost perfection, if it is not mounted on the spindle shaft accurately at the center axis, then the wheel/tire assembly will induce vibrations. When the wheel/tire assembly is not centered properly it induces error in wheel balancing measurements. The difference in axes center with respect to spindle shaft of wheel balancer will result in the errors in determination of wheel rim run-out, the tire force and wheel/tire assembly force variation computation. This centering error becomes dominant with larger wheel/tire assemblies.

In order to avoid errors due to improper centering, modern day wheel balancing

machines are equipped with *Centering Check* mechanism which gives error signal to operator if wheel is not centered on spindle shaft correctly. Such wheel balancer performs centering check of the spindle mounted wheel based on measurement of wheel run-out. The run-out measurements are taken on the wheel which is mounted on the spindle shaft of the wheel balancer. The wheel is then taken out of the spindle shaft and remounted on it. The run-out measurements are taken again after remounting the wheel. The digital signal processor (DSP) of wheel balancers checks the difference between two run-out measurements as per the predetermined threshold for centering check. The wheel balancer can compensate for run-out difference and can also signal operator to remount the wheel. The Hunter wheel balancer DSP9200 is equipped with such *Centering Check* mechanism. [21]

A wide variety of wheel, having different dimensions can be balanced on the same wheel balancing machine. The wheel is mounted on the spindle shaft using the mounting cones. The wheel balancer DSP9200 is provided with multiple cones of varying sizes to accommodate a wide range of wheel sizes. Wheel hub I.D. sits on the mounting cone and the wheel is pressed against this cone by using wing nut. Pressing the wheel against the mounting cone makes wheel to center on the spindle shaft. If the wheel hub I.D. is not perfectly round due to imperfect manufacturing or wear and tear, then even after pressing the wheel against mounting cone and spring plate the wheel will not center.

Centering the wheel on wheel balancer is a challenge that wheel balancer manufacturer is facing. Though they have managed to come up with technologies, such as *Centering Check* and accurate mounting cone, still it is not a perfect system. While working on this research it was realized that centering of wheel on wheel balancer is one area of this entire research that can be improved upon. Hence the efforts were taken to modify the design of current wheel mounting cone and come up with a new design that will improve accuracy of centering.

The high-performance Enkei design Porsche wheel with designation *225/40ZR18* was chosen for testing purpose. This wheel has speed rating ZR, which means it runs at very high speed. Presence of even a small amount of imbalance will induce significant amount of vibrations in this type of high-performance wheel. For these reasons, Porsche wheels were selected for designing new mounting adapter.

4.3.1 Design and Manufacturing of Wheel Balancer Adapter

The wheel mounting cones which are in use currently, hold onto the wheel hub I.D. only at circumference. There is just a line contact between the mounting cones and wheel rim bore. If the leading edge of wheel rim bore which holds onto wheel mounting cone is not perfectly round then it would be difficult to get wheel/tire assembly accurately at spindle shaft center.

The idea for better centering was that 'mounting adapter' and wheel/tire assembly bore has a better and more contact than the traditional wheel mounting cone. The primary objective of designing was to have maximize the contact area between mounting adapter and wheel hub and also to improve centering by precisely manufacturing the cylindric in the design. The adapter which mounts wheel on spindle shaft does not undergo a lot of loading, hence strength is not the primary requirement. Criteria to choose the material for manufacturing was weight and machining ease. The secondary objective of designing was that the hub would be compact, cost efficient and easy to manufacture.

The material that was chosen for manufacturing, which would fulfill the above mentioned requirements, was aluminum. Aluminum is lightweight, it is soft which means easier to machine and it's not very expensive.

The designing process started with measuring dimensions on wheels balancers spindle shaft and wheel rim bore. inside diameter (bore) of wheel mounting adapter sits on the spindle shaft of wheel balancers and outside diameter of pilot or wheel mounting adapter slides into the wheel rim bore. These two diameters were very

critical and important to make accurate centering. The diameter of spindle shaft was measured with outside micrometer to the accuracy of 1/1000th of an inch. Inside diameter of wheel rim bore was measured with Bore-gauge also to the 1/1000th of an inch accuracy. The tolerances were added to the designing part from Automotive Handbook to get the actually machining dimensions. The tolerance for wheel balancer adapter hole, of which nominal diameter is 40mm, was found to be 0mm to +0.025mm [23].

The basic design of wheel mounting adapter looks like a stepped bar with bore in its center. The inside diameter and intermediate diameter was selected as mentioned above. The outside diameter was selected such that it covers most of the wheel balancer flange area. The diameter of wheel balancer flange is 9", so the outside diameter of wheel mounting adapter was selected as 7". The step on the intermediate diameter, the pilot, was selected as 10mm so that the pilot slides all the way inside the wheel rim bore. The step on the outside diameter was selected such that the height of designed part would be roughly 1 inch. The step on outside diameter was selected as 15mm so that the entire designed part height becomes 25mm.

The CAD modeling was executed in a way that it imitates the actual manufacturing operations required to fabricate the design. This can be thought of as commencing with modeling of raw material part, followed by giving finishing cut using extrude command which imitates the facing operation on milling machine and then followed by other manufacturing processes modeled using appropriate commands. The objective of adapting this CAD modeling technique is to determine the feasibility of manufacturing processes required to fabricate this part in addition to extracting the manufacturing drawings from the 3-D CAD model itself. The CAD modeling was carried out in software SolidworkS. The figure 4.7 displays the 3-D isometric view of the CAD modeling of wheel balancer hub.

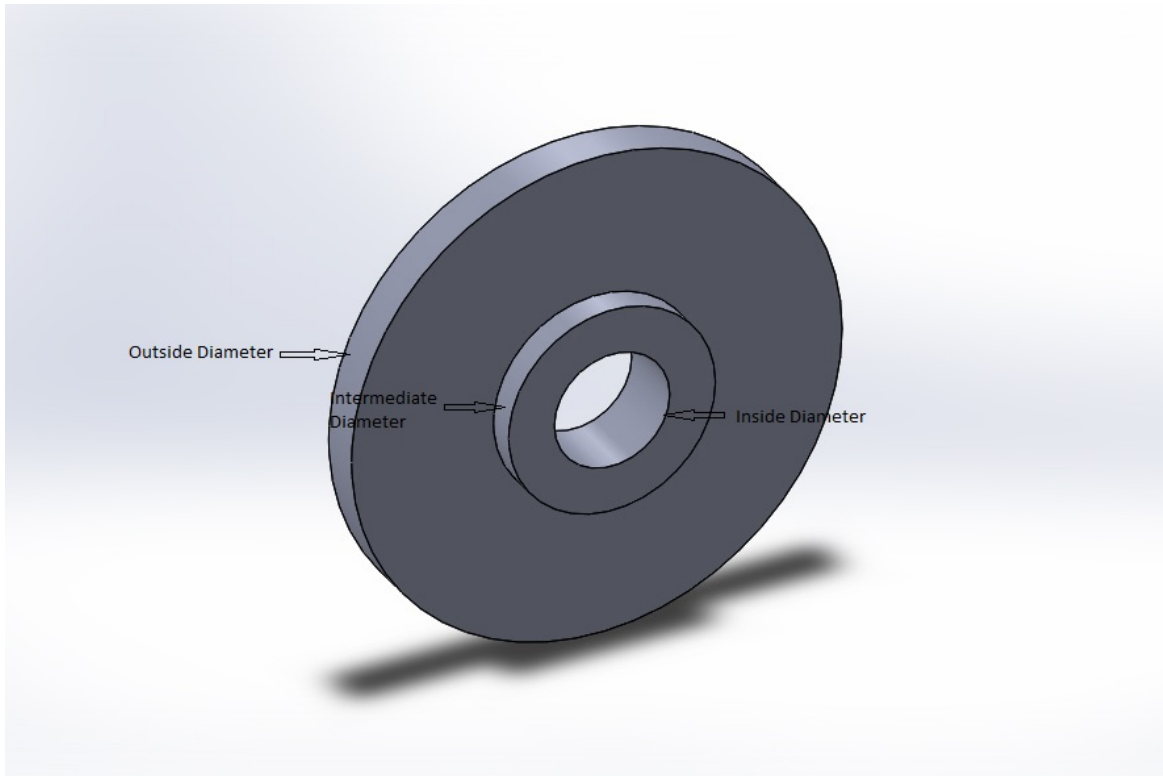


Figure 4.7: Wheel mounting adapter model

The back face of wheel mounting adapter coincides with wheel balancer flange and inside diameter is concentric with spindle shaft. The front face is parallel to the wheel plane and wheel rim bore coincides with the intermediate diameter or the pilot. The intermediate diameter, or the pilot, slides inside the wheel rim bore. The tolerance for the intermediate diameter (71.6mm) is 0mm to -0.019mm. Since the wheel rim bore and pilot have close tolerances, chamfer is provided to aid the centering of rim bore on pilot.

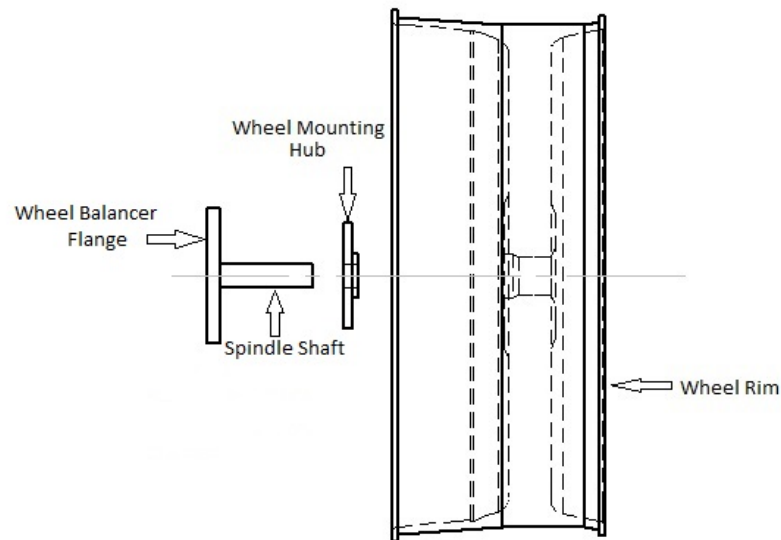


Figure 4.8: Assembly of wheel mounting adapter with wheel rim and spindle shaft

The order of assembly of wheel balancer flange, wheel mounting adapter (pilot) and wheel rim is as shown in figure 4.8. The CAD model of wheel rim is not to the scale and it's only a representation of the order in which assembly is done and not the actual drawing.

The manufacturing of the wheel mounting hub was done on vertical milling machine. The final machined part is shown in figure 4.9. From left to right the figure displays front face (Top view), back face and the side view of the actual wheel balancer adapter.



Figure 4.9: Wheel mounting adapter after manufacturing

4.4 Test Protocol

In this research various operational parameters that can possibly affect the wheel balancing measurements are studied. Slight variation in the standard wheel balancing procedure was added in each undermentioned case to study the effect of that particular parameter on wheel balancing measurement. Following are different cases or the test protocols followed in this research:

1] Effect of tire pneumatic pressure on wheel balancing measurement:

The tire pneumatic pressure is critical in passenger safety. The tire pressure may vary due to weather condition and as a function of time. Tire pressure when tire is hot, as in when vehicle is running on highway or track for long duration is different as compared the tire pressure when tire is cold. Considering all these parameter, it can be stated that tire pneumatic pressure is not always constant and hence it is important to study effect of pressure on wheel balancing. [24]

In this case, firstly, the tire pressure was set to 50 psi. Then the tire was mounted on the wheel balancer. Wheel balancing measurements were taken at this pressure and noted down. Then the tire pressure was reduced to 45 psi and measurements were taken again. In the similar manner wheel balancing measurements were taken and noted down every time by reducing the tire pressure by 5 psi. At each particular

pressure, a set of two wheel balancing measurements were taken to get the confidence on the acquired measurements. The measurements were taken by reducing pressure from 50 psi to 5 psi and another set of measurements were taken by increasing pressure from 5 psi back to 50 psi. In this process the tire was mounted on the wheel balancing machine at the start of this test protocol and was left undisturbed to avoid in undesirable errors.

2] Effect of clocking the wheel/tire assembly on wheel balancing measurements while keeping the tire pressure constant:

In this test protocol tire pressure is kept constant at 35 psi throughout the process. Then the tire is mounted on the wheel balancer and first measurement is taken and noted down. This is the baseline measurement, or the measurement at 0° . At this setting a set of two measurements were taken to check the repeatability of the measurements. Then the wheel/tire assembly was clocked 45° with respect to wheel balancer flange. Clocking the tire on wheel balancer means that dismounting and rotating the wheel/tire assembly with respective wheel balancer flange and then mounting it again on the spindle shaft. Circumference of wheel balancer flange is marked at every 45° and wheel rim marked for reference as shown in figures 4.10 and figure 4.11. Wheel balancing measurements were taken at every 45° clocking till 720° , that is two complete revolution and results were analyzed.



Figure 4.10: Reference markings on wheel rim and wheel balancer flange

Figure 4.11: Close-up of reference marking

3] Effect of tightening torque required for mounting wheel on the machine:

When the wheel is mounted on the wheel balancer, it is pressed against the wheel balancer flange and spring on the spindle shaft with the help of wing nut. The wheel balancer is used by more than one operator and every operator applies different torque or wing nut for tightening.



Figure 4.12: Method to calculate tightening torque

To study effect of tightening torque, in this protocol, wheel balancing measure-

ments were taken by varying the tightening torque applied on wing nut for every set of two measurements, while keeping the constant pressure and without clocking the tire. In this protocol tightening torque was varied from 32 ft-lb (max) to ft-lb at every 2.3 ft-lb (min). Figure 4.12 shows the method adopted to calculate the tightening torque applied on wing nut. Arm length of wing nut arm is 137 mm and force applied of the wing nut arm is measure as shown in the figure 4.12.

4] Effect of off-setting tire/wheel assembly using metal shims on wheel balancing measurements:

As mentioned before, accuracy of wheel balancing measurement depends on how accurately the wheel is mounted and centered on the spindle shaft. The wheel is mounted using wheel mounting cone and pressed against wheel balancer flange. If this flange or wheel rim face which is touching this flange is damaged, then it will not center on the spindle shaft properly which will affect the balancing measurement. To simulate this condition metal shims were placed between wheel rim flange and wheel balancer flange as shown in figure 4.13.



Figure 4.13: Offsetting wheel mounting cone with metal shims

In this protocol, first measurement was taken without putting metal shim. This is baseline measurement. Then metal shim of 0.01mm is put between wheel mounting

cone and flange and measurements are taken. Measurements are repeated by increasing shim thickness by 0.01mm for each measurement. Shim thickness is varied from 0.01mm to 0.1mm and measurements are noted down.

5] Sensitivity test of dataset arm by giving incorrect tire width input:

Input of tire dimensions are provided to the wheel balancer computer by using the two dataset arms. Tire width and radius is provided as a input by placing the dataset arm in the weight emplacement locations and hitting the foot pedal. In this protocol the input of tire width is altered, and incorrect width value is set using dataset arm and measurements are taken. For each new measurement in this protocol, the dataset arm input location is shifted horizontally by 10mm and wheel balancing measurements are taken.

6] Sensitivity test of dataset arm by giving incorrect tire radius input:

In this protocol the input of tire width is altered, and incorrect radius value is set using dataset arm and measurements are taken. For each new measurement in this protocol, the dataset arm input location is shifted radially by 10mm and wheel balancing measurements are taken.

7] Comparison of wheel balancing measurement with newly designed wheel mounting hub:

As mentioned in section 4.3, new wheel balancing hub is designed in this research that will replace the conventional wheel mounting cone and improve the accuracy of centering. In this protocol, wheel balancing measurements are taken on this new wheel mounting hub and results are compared with the wheel balancing measurements taken while using conventional wheel mounting cone.

4.5 Procedure

Measurements were made on a Hunter DSP-9200 wheel balancing machine shown in figure 4.1 in the research lab of the Motorsports Research Building at the University of North Carolina at Charlotte. The standard procedure to take wheel balancing

measurement has been followed during this research except that the procedure varies to some extent in order to follow each of the above mentioned test protocols.

Pressure details:

In order to get the standardized result, the pneumatic pressure on the test wheels was kept standard for all measurements except for the test protocol where tests are run to study the effect of pressure on wheel balancing. The tire pneumatic pressure was always set to 35psi at 72° F.

The zero offset weight function:

The multiple wheel balancing measurements are taken to study one test protocol. In each measurement correction weight magnitude and its location is noted down and its variation is analyzed. It is important to have some amount of imbalance in wheel to study the variation in its location. Therefore, to avoid getting null reading, test wheels are purposefully offset in two planes with 10g (0.5oz) weight.

Angular marking on test wheel and laser angle measurement:

After offsetting wheel, a sample measurement is taken. The rim flange of the test wheel is marked on flange to + or - 40° about the mean correction weight location. It is observed from the measurements that variation in wheel balancing weight location is about 40°. A span of 80° is provided to make sure that measurements always fall inside the marked area. Calibrated wheel with rim marked in on degree increment at rim flange is shown in the figure 4.14.



Figure 4.14: Wheel calibration

Even if the wheel is calibrated perfectly, it is difficult to identify TDC position on wheel accurately and read the angle measurements(calibrated markings) just by naked eyes. To avoid this error a laser was mounted to the balancing machine with a Manfrotto arm [25] to increase the angular measurement accuracy as shown in figure 4.15 and figure 4.1. It was directed to the inside of the rim where a wheel weight is attached as it can be seen in figure 4.15. The figure 4.16 shows the close up of the rim flange marked in one degree increment with laser pointer pointed at it for measurements.

Measurement machine's calibration:

The Hunter DSP9200 has a self check for calibration; however, to assure the greatest accuracy, we performed a manual calibration. The Operators Manual [20] describes the process whereby a calibration weight is attached to the machine hub and run in a forward and reverse position as shown in figure 4.17. The machine is placed in a special calibration mode and run through a sequence of operations. In the end, there



Figure 4.15: Laser pointer mounted on wheel balancer



Figure 4.16: Wheel calibration and laser pointer close up

was no measurable change to the calibration of the machine during the testing. This operation is also explained in section 2.4.



Figure 4.17: Calibration of the machine

Standard balancing procedure followed:

- 1] Test wheel is pumped to standard pressure.
- 2] Wheel is mounted on the spindle shaft using wheel mounting cone or the specially designed wheel mounting adapter and pressed against wheel balancer flange using wing nut.
- 3] Wheel is then checked for imbalance, and if found balanced, offset imbalance weight is added to the wheel as mentioned above.
- 4] Test wheel is calibrated. Rim is marked on in the increment of one degree on

rim flange.

5] Input of wheel dimension, that is the weight plane location is provided to the wheel balancer by using dataset arm.

6] Once all inputs are set, the safety hood is lowered to run a wheel balancing measurement. When the measurement is complete, wheel stops rotating and safety hood can be raised. The measurements are displayed on the control panel.

Note that this procedure is used for all test protocol with some variation required for that particular protocol.

CHAPTER 5: RESULTS AND DISCUSSION

Measurements are taken in a way explained in test protocol section. Results of these test protocols are discussed in this chapter. In each test measurement, four primary inputs were noted as follows: 1] Magnitude of weight to be placed in plane 1 rim flange. This weight is called *Inner Weight* since it is closer to the machine, 2] Angular location of the inner weight called, *Inner Angle*, 3] Magnitude of weight to be placed in plane 2 location. This weight is called *Outer Weight* since it is away from the machine, 4] Angular location of the outer weight called, *Outer Angle*.

5.1 Test Protocol 1: Effect of Pressure

This test was run on 225/40 ZR 18 (Porsche front tire) and 265/35 ZR 18 (Porsche rear tire) tires. Figure 5.1 displays the plot of balancing weight against tire pneumatic pressure and figure 5.2 displays the plot of location of balancing weight against tire pressure for the test tire 225/40 ZR 18. Figure 5.3 and figure 5.4 displays similar plots for test tire 265/35 ZR 18. It can be observed from these plots that effect of pressure on balancing weight and its location is predominant at extreme low pressures. The magnitude of balancing weight remains constant till the tire pressure of 25 PSI. For test tire 225/40ZR18, below 25 PSI the magnitude of balancing weight goes on reducing, whereas for test tire 265/35ZR18, the balancing weight magnitude first decreases and then increases. It can be concluded that, the effect of pressure on magnitude of wheel balancing weight is dependent on wheel geometry and its predominant in low tire pressure region. Fluctuation in balancing weight location is about 10-15° and similar to the case with balancing weight magnitude, effect of pressure on weight location is predominant in lower tire pressure region.

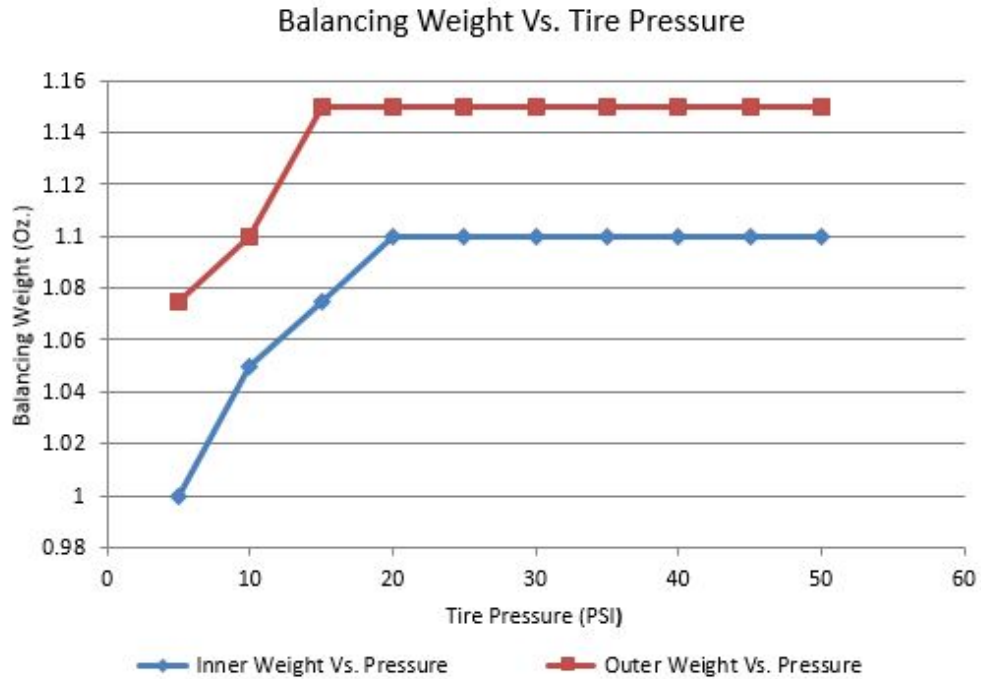


Figure 5.1: Test tire:225/40ZR18 - effect of pressure on balancing weight

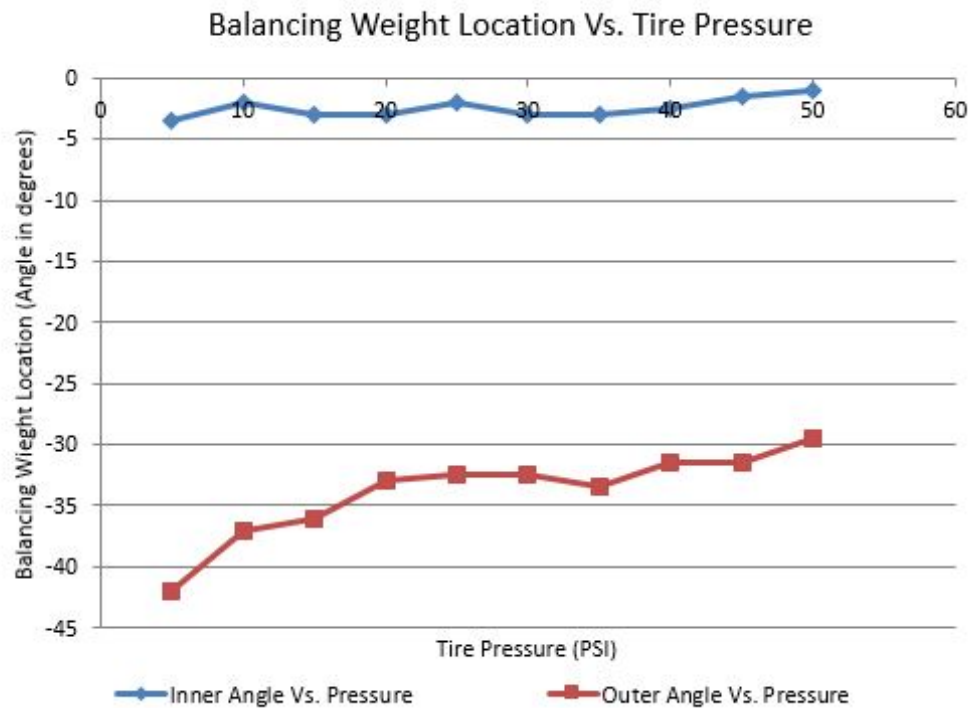


Figure 5.2: Test tire:225/40ZR18 - effect of pressure on location of balancing weight

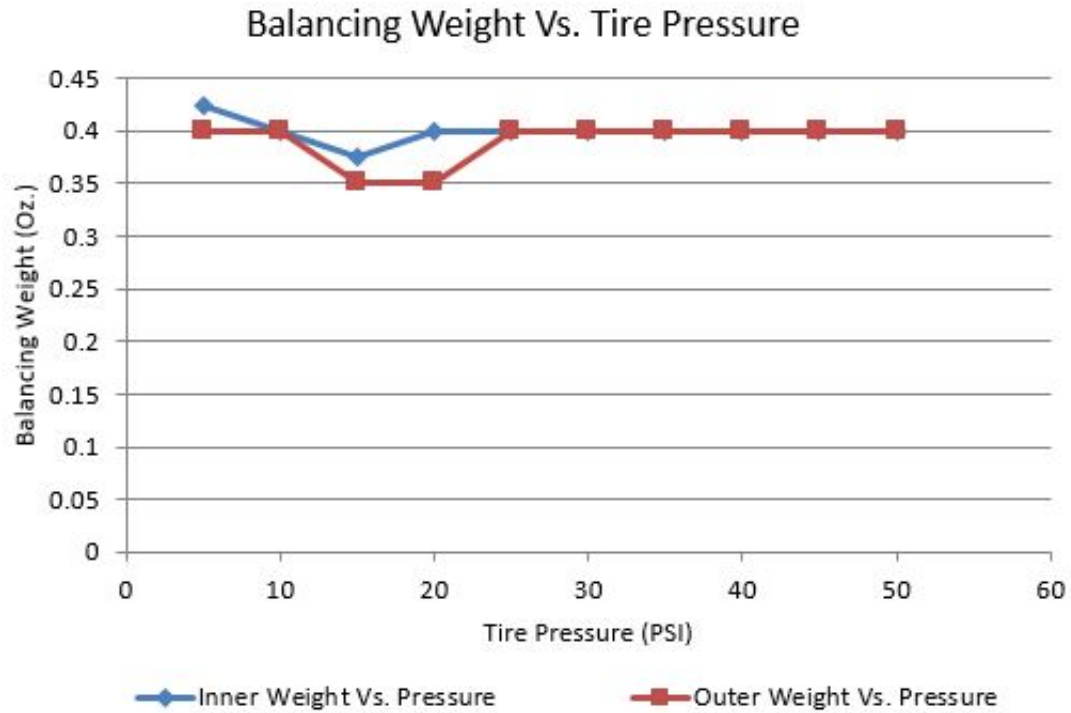


Figure 5.3: Test tire:265/35ZR18 - effect of pressure on balancing weight

5.2 Test Protocol 2: Effect of Clocking

Clocking is the process of dismounting or loosening the test wheel from spindle shaft, rotating it to a certain angle with respect to its original position and then mounting or tightening it again on the spindle shaft. In this test protocol clocking is done at every 45° and measurements are recorded. For most of the measurement wheel is clocked up to 360° (2 revolutions) and few measurements are taken up to 1440° (4 revolution) to study the trend of measurements change with clocking.

Theoretically, wheel balancing measurements should not change with clocking as imbalance in wheel/tire assembly is fixed but it is observed from the measurements that it changes to certain extend with clocking. This could be due to the residual imbalance present in the spindle shaft drive assembly of the machine. The cause of this residual imbalance is required to study in details. Figure 5.5 and figure 5.6 displays the plots for effect of clocking on balancing weight and its location respectively for test

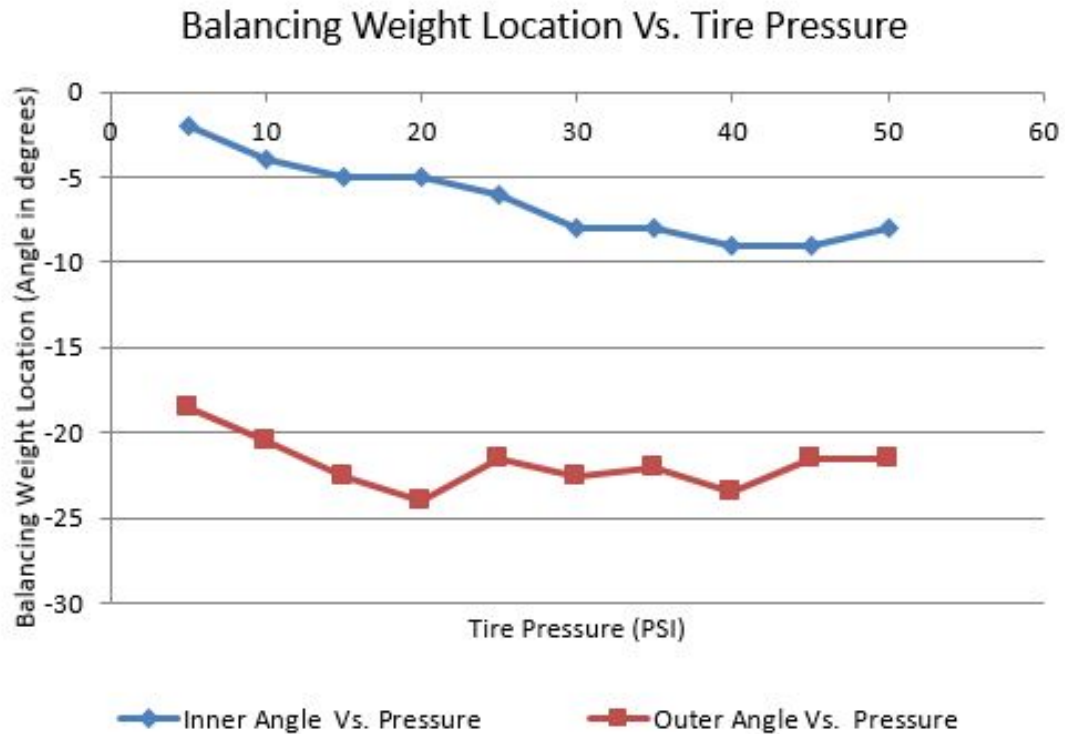


Figure 5.4: Test tire:265/35ZR18 - effect of pressure on location of balancing weight

tire: 225/40 ZR 18. Figure 5.7 and figure 5.8 shows similar graphs for test tire 255/40 ZR 17. Both these test tires shows similar sinusoidal trend. Variation in balancing weight is about 0.35 Oz whereas variation in its location is about 45° .

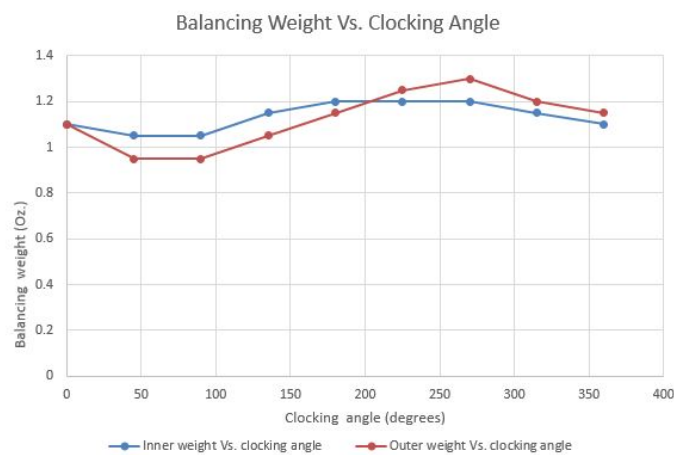


Figure 5.5: Test tire:225/40ZR18 - effect of clocking on balancing weight

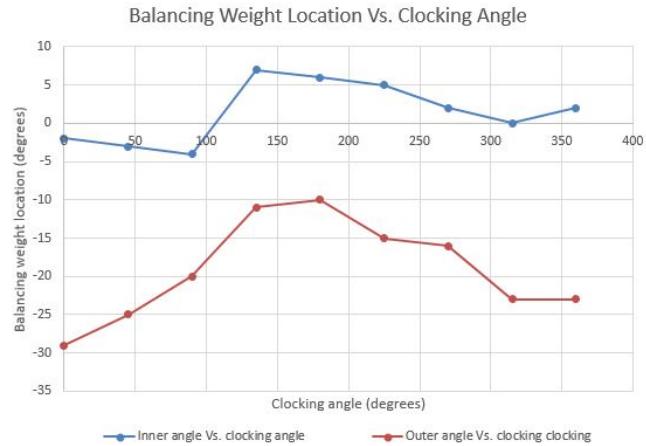


Figure 5.6: Test tire:225/40ZR18 - effect of clocking on location of balancing weight



Figure 5.7: Test tire:255/40ZR17 - effect of clocking on balancing weight



Figure 5.8: Test tire:255/40ZR17 - effect of clocking on location of balancing weight

Test tire 205/40 ZR17 was tested on wheel measurement run with 456° for 4 revolution i.e. 1440°. Figure 5.9 displays the variation in inner and outer balancing weight magnitude. It can be observed from these plots that measurements in all four revolutions follows a similar trend. Figure 5.10 displays the trend of change in location of wheel balancing weight for test tire 205/40 ZR 17 for four revolution.

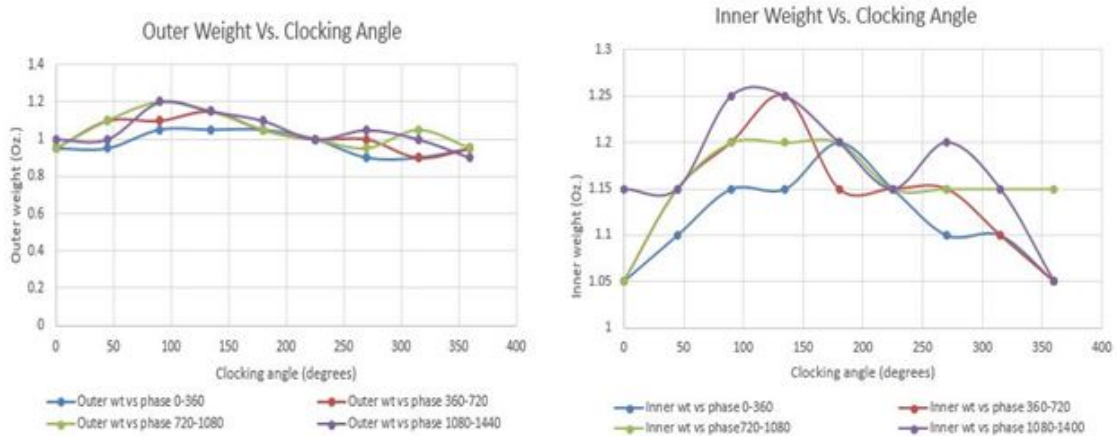


Figure 5.9: Test tire:205/40ZR17 - effect of clocking on balancing weight for four revolution

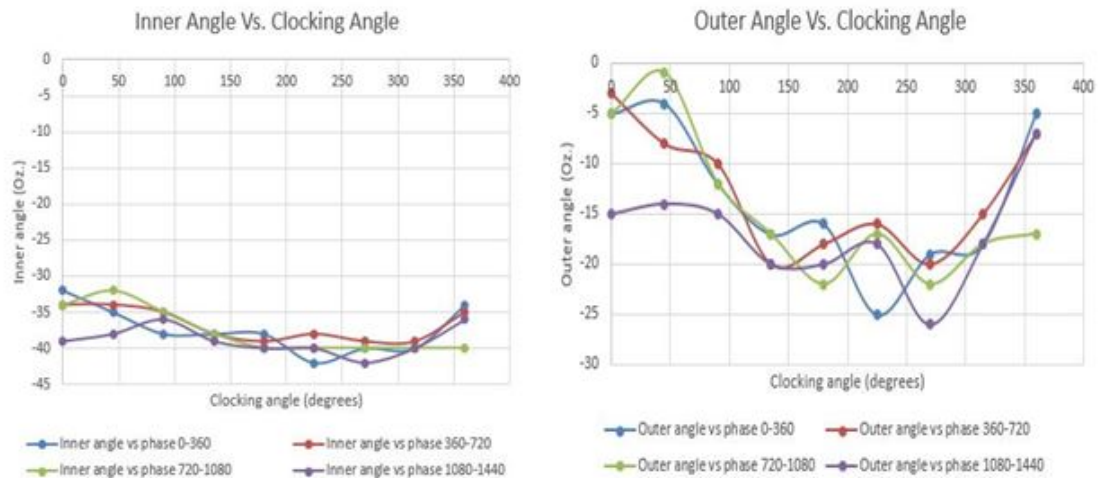


Figure 5.10: Test tire:205/40ZR17 - effect of clocking on location of balancing weight for four revolution

5.3 Test Protocol 3: Effect of Tightening Torque

In this test effect of tightening torque on wheel balancing measurements is studied. DSP9200 has an inbuilt function which can detect if wheel is not mounted on spindle shaft or if it is not tight enough, and if this is the case then it displays a message 'LOOSE' on control panel screen. It is found in this test if the applied tightening torque on the wheel is less than or equal to 2.3 ft-lb, then machine displays 'LOOSE' message.

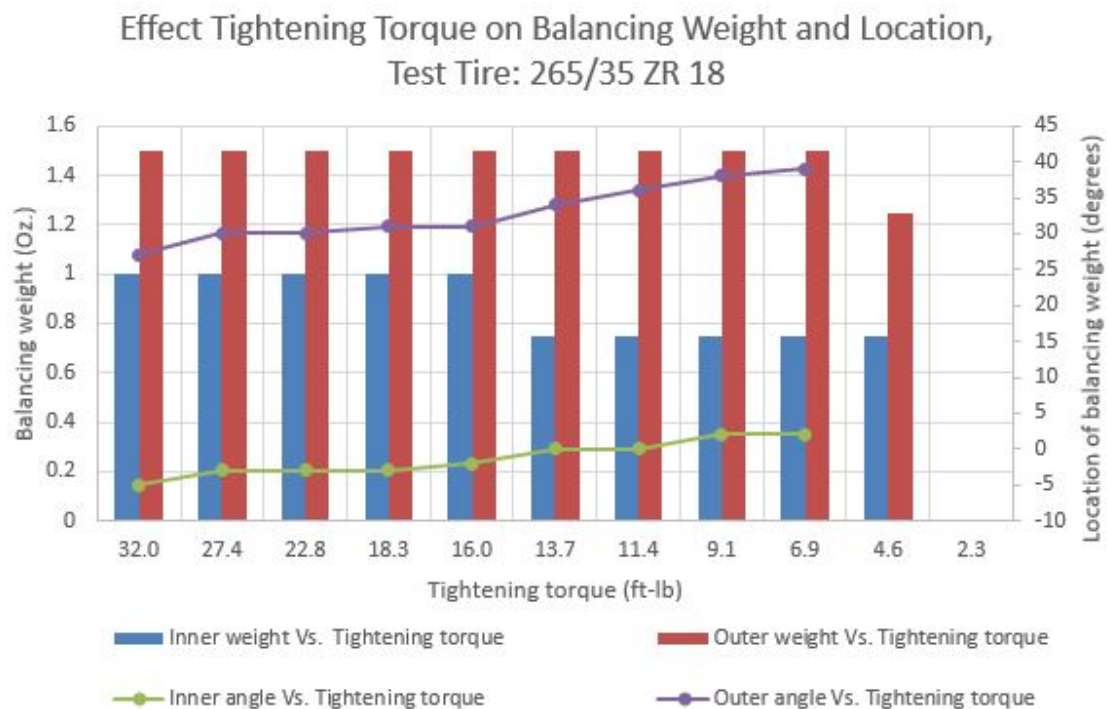


Figure 5.11: Test tire:265/35ZR18 - effect of tightening torque on wheel balancing measurements

Plot shown in figure 5.11 explains the effect of tightening torque for test wheel 265/35 ZR 18. Columns indicates the magnitude of wheel balancing weight and lines with markers indicates the value of balancing weight location(angle). Figure 5.12 displays similar plot for test tire 225/40 ZR 18. Both these plots shows similar trends, which confirms the results. For tightening torque 16 ft-lb or less, machine gives erroneous values but it still does not displays 'LOOSE' message on control panel. It

can be observed from both the plots that there are less datapoints for location of balancing weight(line) than magnitude of balancing weight(bars). Reason for this is that, the wheel slips on the spindle shaft for lower tightening torque thereby making location of wheel balancing weight irrelevant even if machine displays balancing weight magnitude and location on screen. In ideal case, at such low tightening torque when wheel slips on the spindle shaft, machine should display 'LOOSE' message on screen.

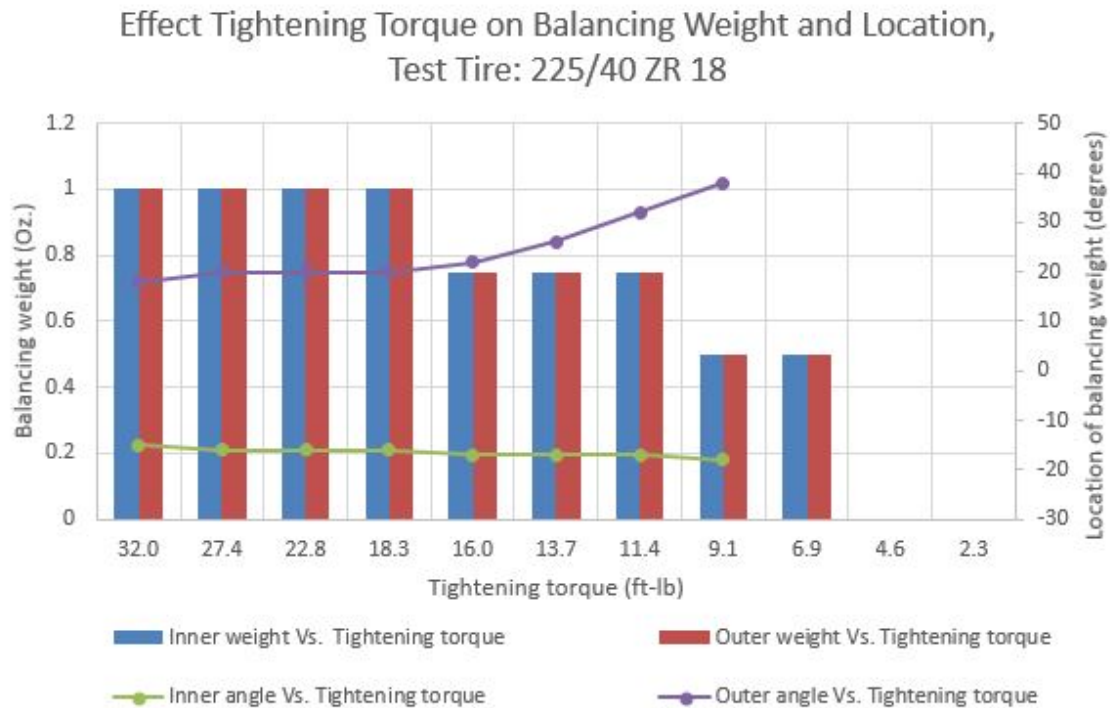


Figure 5.12: Test tire:225/40ZR18 - effect of tightening torque on wheel balancing measurements

5.4 Test Protocol 4: Effect of Wheel Offset

In this test protocol, effect of offsetting wheel on spindle shaft is studied. Metal shim is placed between wheel balancer flange and wheel rim hub. Figure 5.13 displays the effect of shim thickness on wheel balancing measurements. First column refers to measurement without putting shim, next measurements onwards shim thickness is increased by 0.01 mm every time up to 0.1 mm. Influence of shim thickness becomes predominant after 0.06 mm.

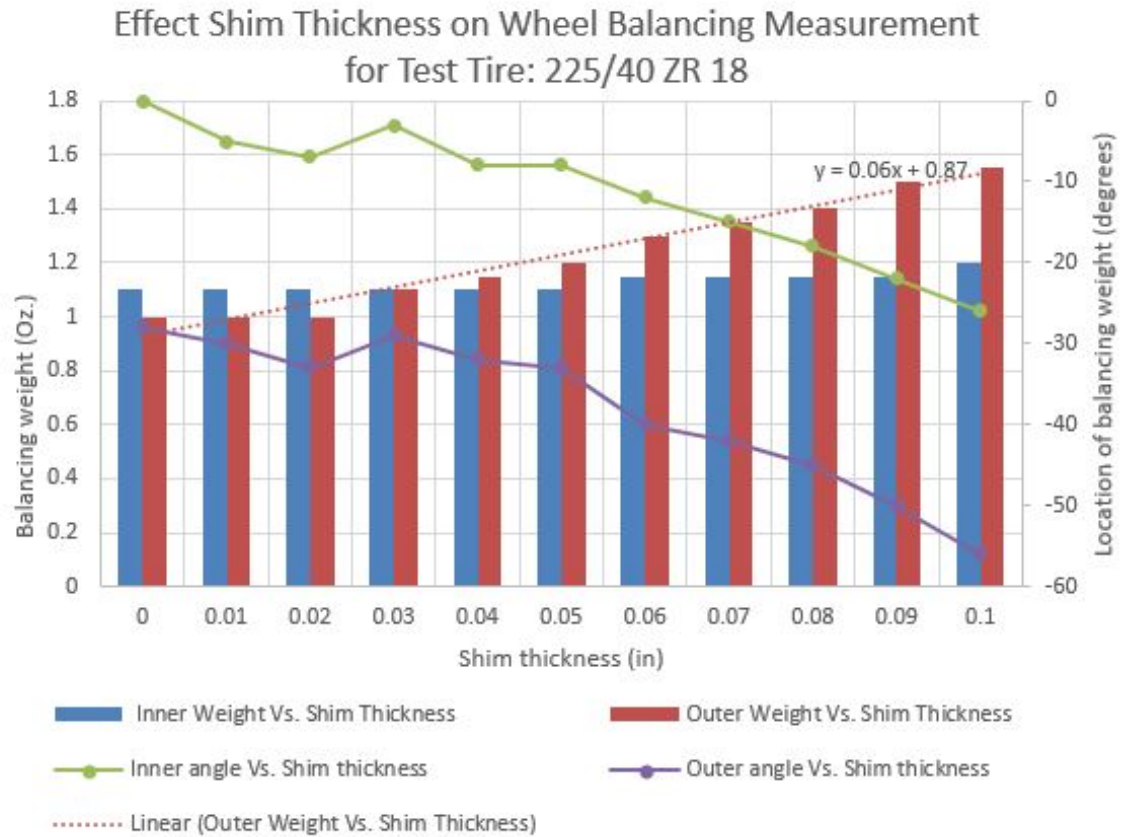


Figure 5.13: Test tire:225/40ZR18 - effect of offsetting wheel with metal shims of different thickness

Angular measurement of balancing weight location is very fluctuating for shim thickness lesser than 0.06 mm. This fluctuation is under 10°. For thickness more than 0.06 mm measurement follows linear trend. Magnitude of wheel balancing weight also keep on increasing after shim thickness of 0.06 mm.

Another set of measurement was taken by clocking shim of 0.06 mm thickness 45° every time up to 360°. This simulates the case if there is a protrusion on wheel balancer flange. Figure 5.14 shows the variation in balancing weight with clocking shim. Figure 5.15 shows variation in location of balancing weight with clocking shim. Since outer weight plane of wheel is away from the wheel balancer flange where shim is placed, effect of offsetting in this plane is more.

Balancing Weight(Oz.) Vs. Clocking Angle(degrees) for Shim Thickness 0.06mm

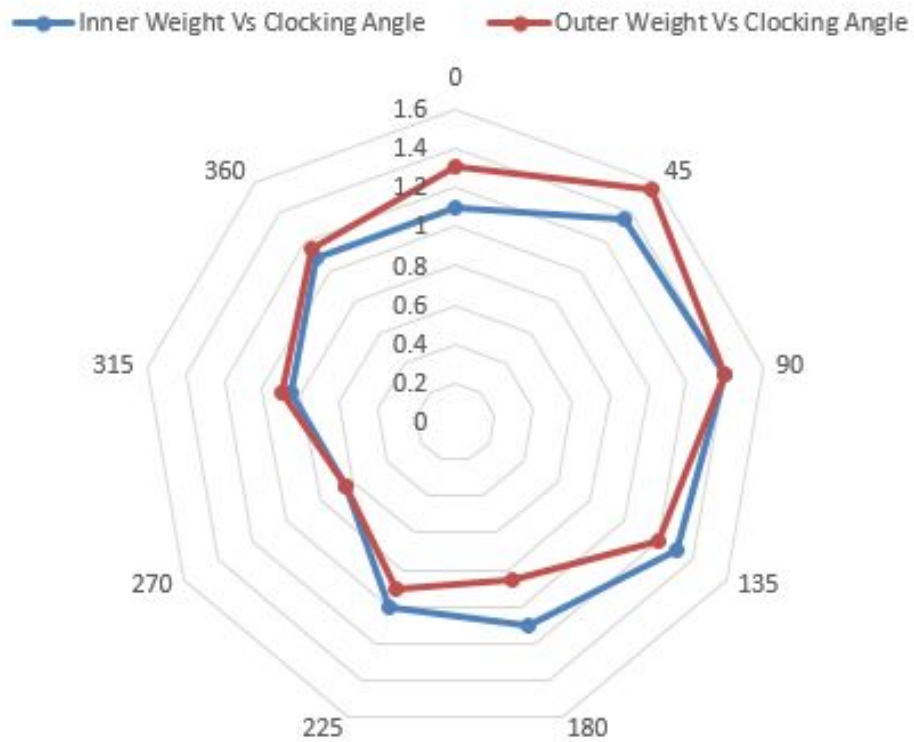


Figure 5.14: Test tire:225/40ZR18 - variation in balancing weight while using 0.06 mm thick metal shim offset

Location of Balancing Weight(degrees) Vs. Clocking Angle(degrees) for Shim Thickness 0.06mm

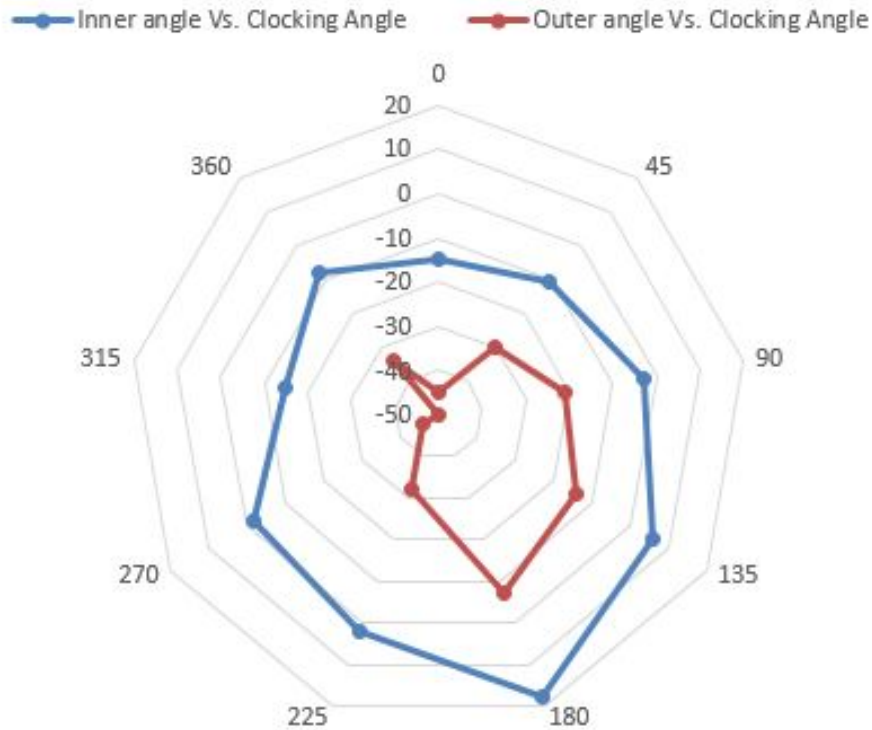


Figure 5.15: Test tire:225/40ZR18 - variation in location of balancing weight while using 0.06 mm thick metal shim offset

5.5 Test Protocol 5: Axial Sensitivity of Dataset Arm

Two different set of measurements are recorded in this test protocol. In one set, inner dataset arm is offset from the wheel rim flange. This offset is increased for each measurement by 10 mm up to 100 mm. Figure 5.16 shows this set of measurement on test tire 225/40 ZR 18. In another set of measurements, outer dataset are is offset from wheel rim flange and similar to previous measurements set this offset is increased each time by 10 mm up to 100 mm. Offsetting dataset arms axially, reduces the magnitude of balancing weight. Effect of both set of measurement is similar. As it can be observed from the plot that the offset in inner dataset arm has more effect on outer plane imbalance weight and location measurements and vice versa for

outer dataset arm. By offsetting dataset arms outwards, input of wheel width to the wheel balancing machine is increased therefore the magnitude wheel balancing weight goes on decreasing. This effect can be confirmed from the mathematical equation explained in chapter 3. Larger the wheel wheel width (distance between the weight plane locations), lesser is the magnitude of balancing weight required therefore it is preferred to put balancing weight at the outermost location possible on wheel rim. Variation in angular location of balancing weight is very less (less than 10°). Effect on location of balancing weight is more evident for offset of 50 mm or more.

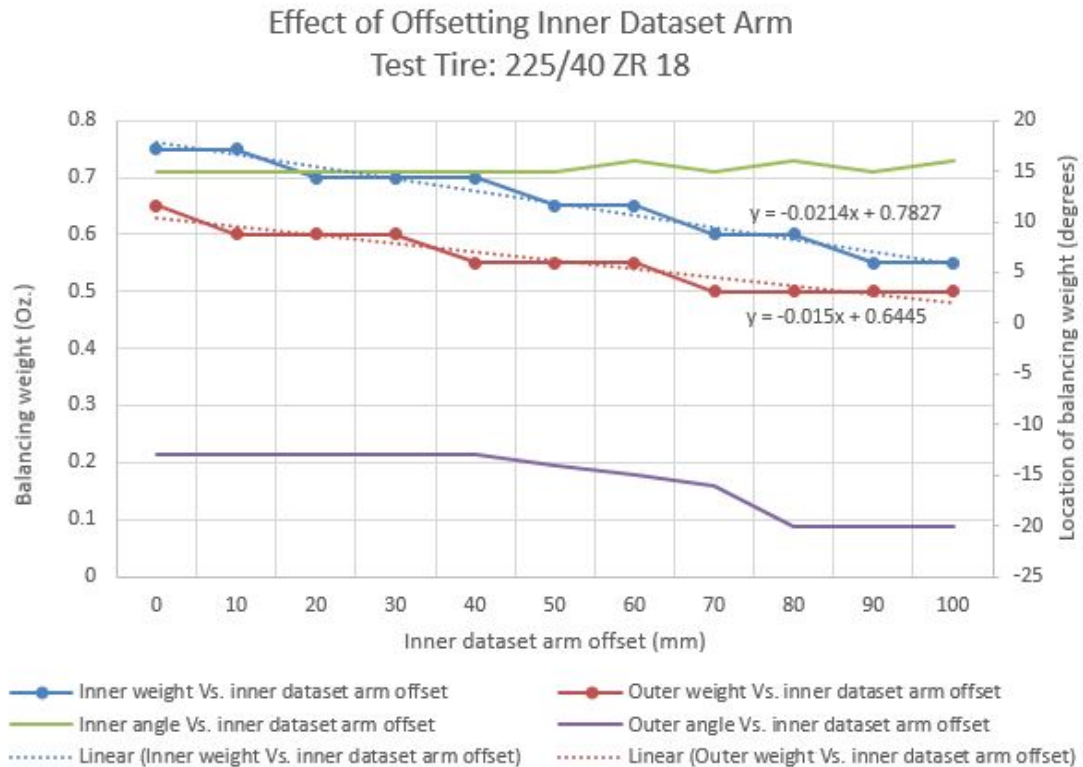


Figure 5.16: Test tire:225/40ZR18 - effect of offsetting inner dataset arm

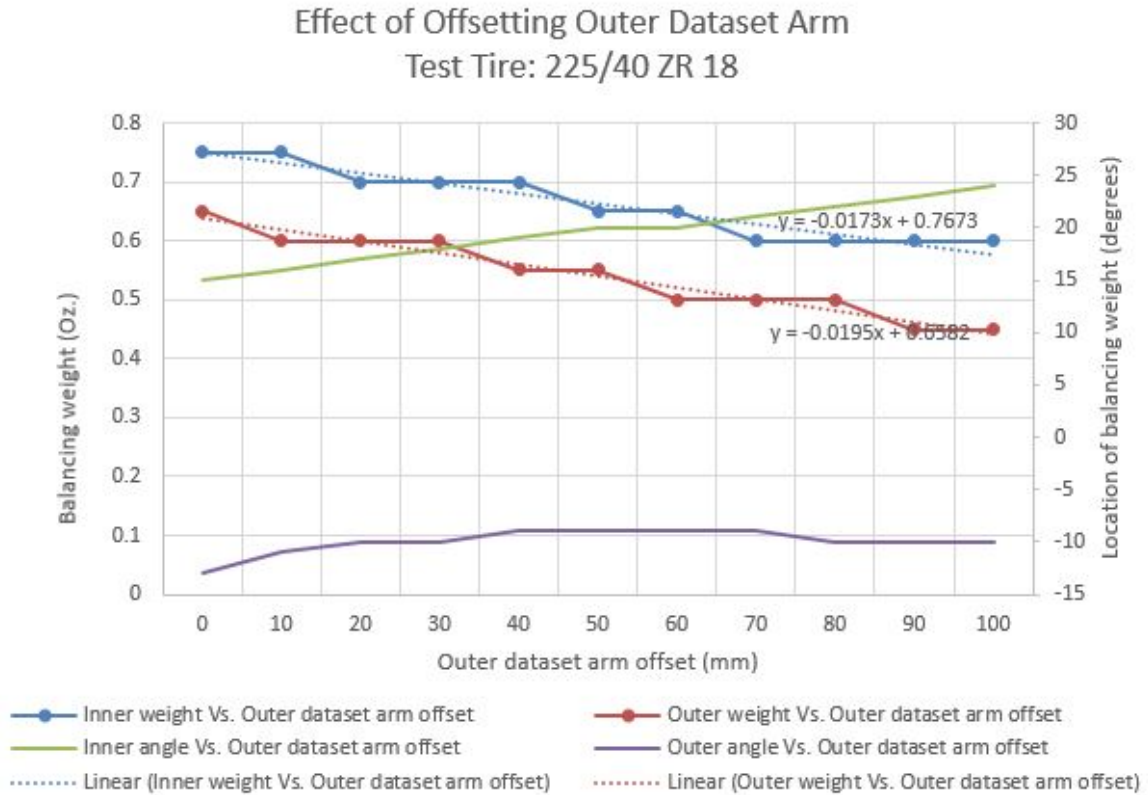


Figure 5.17: Test tire:225/40ZR18 - effect of offsetting outer dataset arm

5.6 Test Protocol 6: Radial Sensitivity of Dataset Arm

In this test protocol, dataset arms are offset from wheel in radial direction (inwards), that is wheel radius input is decreased by 10 mm in every measurement up to total decrement of 100 mm. Figure 5.18 displays the results of offsetting dataset arms radially. Theoretically, lower the radius higher the magnitude of balancing weight. This is confirmed from the plot in figure 5.18. As the radial offset is increased, balancing weight goes on increasing. Location of balancing weight is not changed much by offsetting dataset arms radially. Variation in magnitude of balancing weight is about 0.3 Oz.

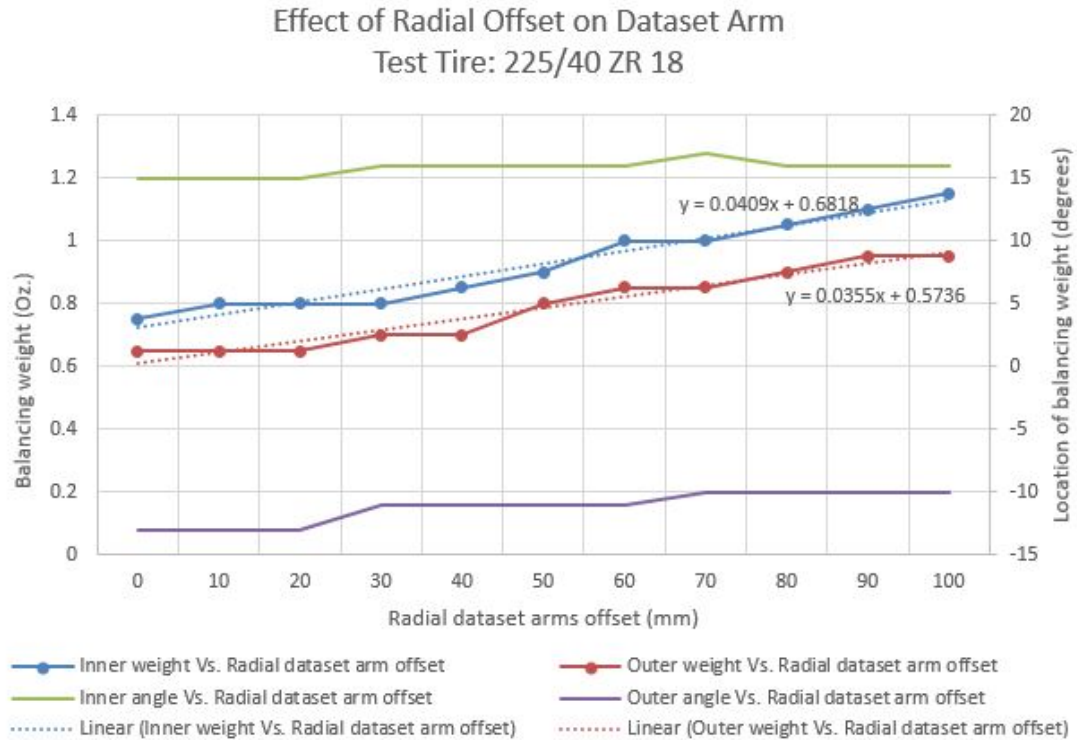


Figure 5.18: Test tire:225/40ZR18 - effect of offsetting dataset arm radially

5.7 Test Protocol 7: Performance of Specially Designed Wheel Mounting Adapter

As described in the results of section 5.2, the magnitude of balancing weight and its location changes with clocking of wheel with respect to wheel balancer. Efforts are taken in this research to improve the centering of wheel on spindle shaft. It is proposed that by improving centering, error due to clocking can be reduced and thereby accuracy of the machine can be increased. For better centering, a new adapter was designed and manufacture to replace the conventional wheel mounting cone. This section includes result of performance of this newly designed adapter.

Figure 5.19 displays the results of test of clocking wheel and adapter together for 720°. Lines with markers indicates the variation in magnitude of wheel balancing weight and line without markers indicates variation in balancing weight's location. The variation in balancing weight is about 0.15 Oz.The variation in the location of balancing weight is about 8°. For the same test tire, variation in balancing weight

was about 0.2-0.35 Oz. as it was observed in section 5.2 and variation in balancing weight location was 12° . Sinusoidal wave form of wheel balancing measurements is still observed in this new measurements. Hence the error due residual imbalance which was observed in measurements before using new adapter is not completely eliminated, however, the variation is reduced to certain extend.

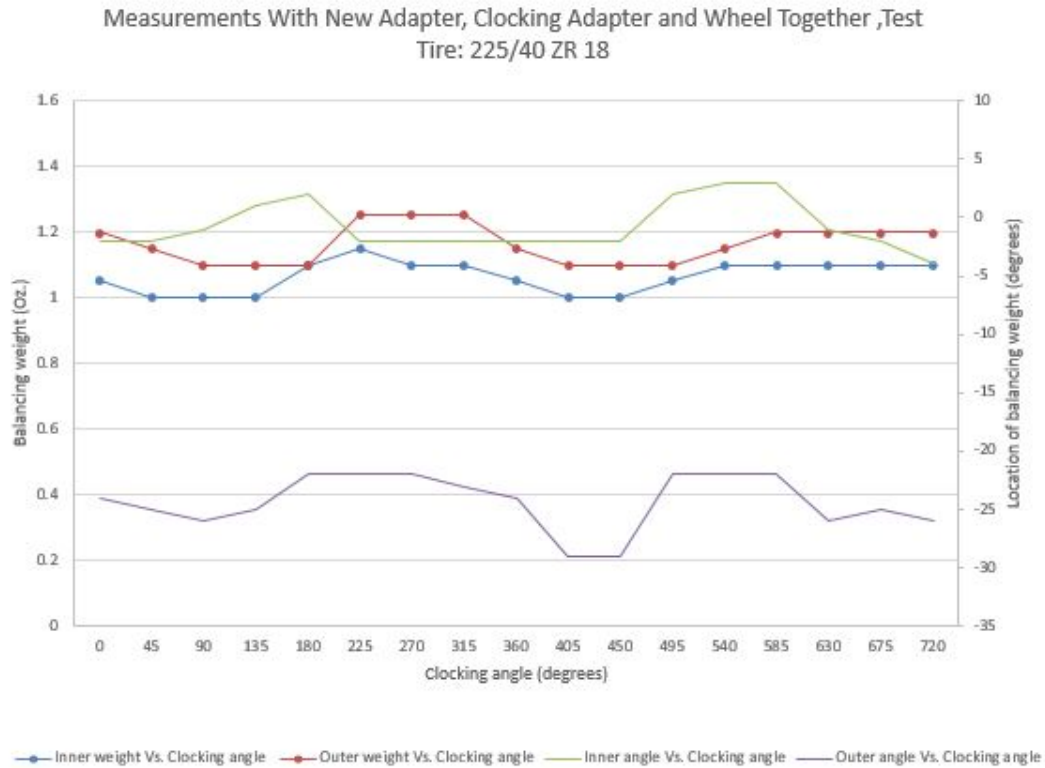


Figure 5.19: Test tire:225/40ZR18 - measurements with new adapter, clocking wheel and adapter together

In another set of measurements the wheel was clocked alone while keeping the wheel mounting adapter with wheel balancer flange to find out which of these two cases give better measurements. Figure 5.20 displays the results of this set. It can be observed that measurements of this set are more rough as compared to measurements in shown in figure 5.19. The adapter and wheel rim bore has a very close tolerance, which makes it difficult to clock tire with respect to adapter. Measurements taken by clocking wheel and adapter together with respect to wheel balancer flange shows

smoother curves and it also eliminate the risk of damaging the adapter. To get the best results, it is recommended that adapter and wheel are clocked together.

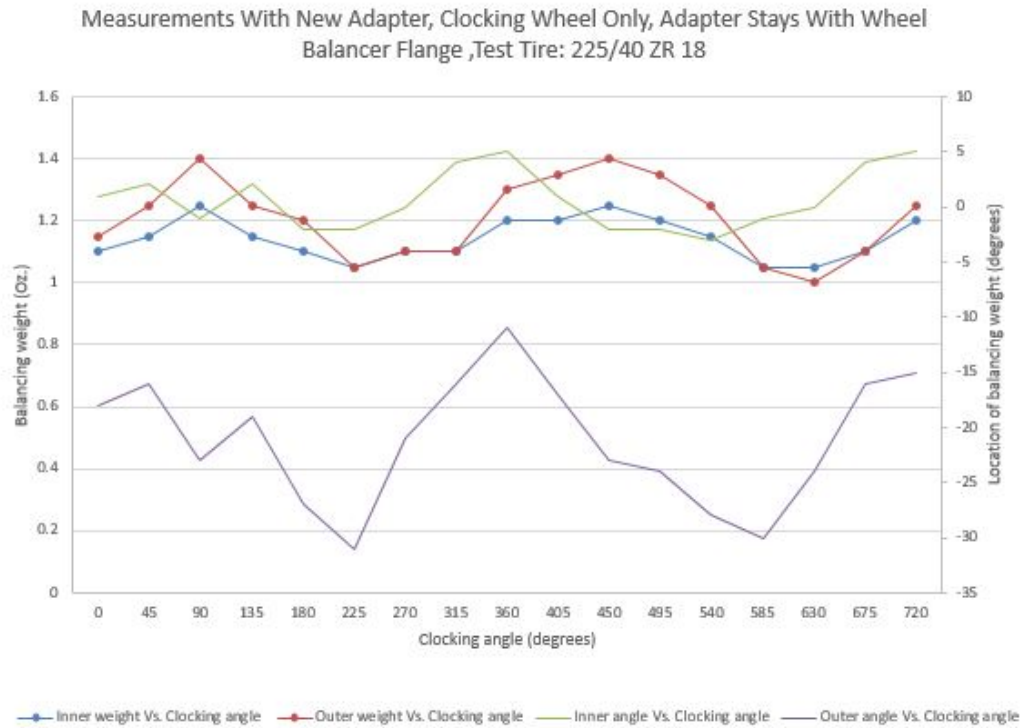


Figure 5.20: Test tire:225/40ZR18 - measurements with new adapter, clocking wheel alone

Figure 5.21 and figure 5.22 displays the measurement results for the two above mentioned cases. It can be observed in these two images as well that clocking adapter and wheel together gives better measurement than clocking wheel alone. In comparison with results for test tire 225/40 ZR 18, results for test tire 265/35 ZR 18 are more fluctuating and variation in balancing weight and its location is more in case of test tire 265/35 ZR 18. The adapter was newly manufactured for the measurements with test tire 225/40 ZR 18, hence there was no effect of wear on these measurements. After test tire 225/40 ZR 18, many more measurements were taken using new wheel mounting adapter. In this process, the adapter was severely worn off by the time the last measurement on test tire 265/35 ZR 18 was recorded. Due to the wear and tear

in new wheel adapter, the measurements for test tire 265/35 ZR 18 are so fluctuating. Even in case of measurements for test tire 265/35 ZR 18, measurements when wheel and adapter are clocked together are smoother than the later case which confirms with the proposition mention prior in this section.

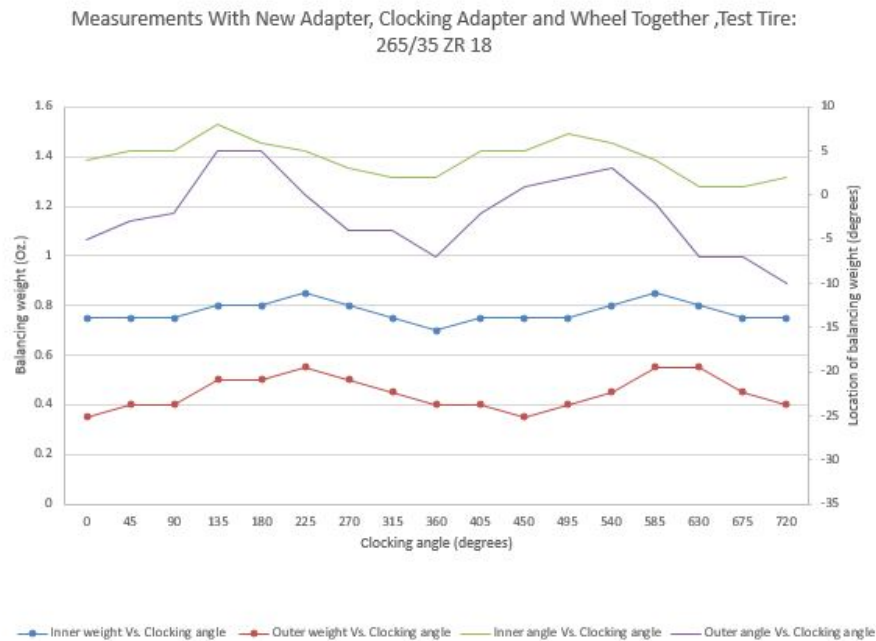


Figure 5.21: Test tire:265/35ZR18 -measurements with new adapter, clocking wheel and adapter together

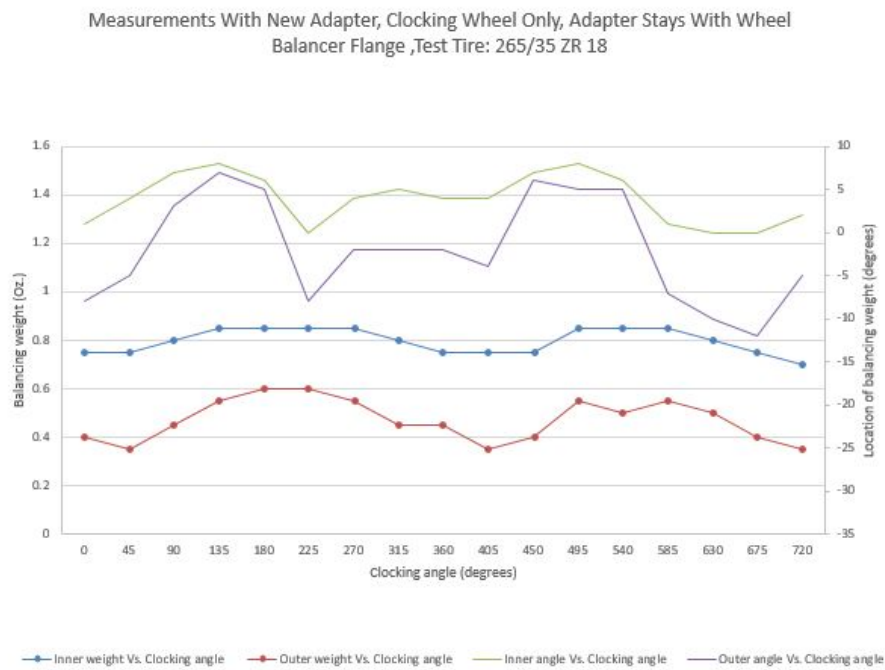


Figure 5.22: Test tire:265/35ZR18 - measurements with new adapter, clocking wheel alone

CHAPTER 6: CONCLUSION AND FUTURE SCOPE

6.1 Conclusion

Main focus of this thesis is to evaluate the various operational variable that influences the wheel balancing parameters. Research started with extensive study of wheel balancing measurements for numerous test tires. Aspects such as tire's pneumatic pressure, clocking of wheel/tire assembly, tightening torque applied while mounting wheel on wheel balancer, offset in wheel while mounting wheel on wheel balancer, axial and radial sensitivity of input dataset arm of wheel balancer was studied during this research. Findings of these tests are highlighted in this chapter.

While studying effect of pressure, many tires were tested while varying the pressures during measurements. It was observed that for a wide range of working tire pressure, wheel balancing measurements are constant. Although it can be concluded that at extreme low pressure, that is lower than 25 PSI tire pressure, wheel balancing pressure fluctuates. Required balancing weight for lower pressure is lower than the balancing weight required at optimum pressure. This is due to slight deformation in tire shape at extreme low pressures.

During study of effect of clocking on wheel balancing measurements, it was observed that wheel balancing measurements follows an abnormal sinusoidal trend contradicting the theory of imbalance. This fluctuation is due to the residual imbalance in wheel balancer DSP9200. Effort are taken in this research to reduce this error in measurements. It was proposed that the error can be reduced by improving centering of the wheel on wheel balancer spindle shaft. A special wheel mounting adapter was designed and manufactured to improve centering. This adapter makes a plane-contact

as compared to conventional wheel mounting cone which makes only a line-contact with wheel rim bore. It was proved to be a better alternative to conventional cone as it reduced the fluctuation in wheel balancing measurements. This new adapter is made up of aluminum, which is comparatively soft metal and it has very close tolerance with wheel rim bore. These induced a lot of wear in adapter over few measurements. Quality of measurements went of degrading after every measurement on this new adapter due to the wear and tear.

Sensitivity of dataset arm was tested by offsetting dataset arm from the wheel rim flange, which is the balancing weight location. When offsetting dataset arm axially outwards, magnitude of wheel balancing weight keep reducing and when offsetting dataset arm radially inwards the magnitude of wheel balancing weight increases. This confirms with the theoretical mathematic equation of wheel balancing as described in chapter 3.

6.2 Future Scope

Work presented in this thesis states that there is a residual imbalance in the wheel balancer DSP9200. In future this part can be researched on in depth to find out the exact cause of this residual imbalance and amount of residual imbalance. Various methods can be researched on and implemented to eliminate this residual imbalance.

An adapter was designed to mount wheel on wheel balancer which was proposed to improve the centering. But due to wear and tear of aluminum adapter, it resulted into erroneous data over the period time. There is a lot of scope to improve the design of wheel mounting adapter to perfection. Design of experiment method can be used to achieve the best design of wheel mounting adapter. Cost of manufacturing this adapter on large scale can be estimated and feasibility of using this adapter in auto industry for balancing high performance tire can be evaluated. Wheel balancer DSP9200 is equipped with quick calibration technology but in future machine should be checked for calibration using proper calibration tool to see if residual imbalance

can be reduced/eliminated by that.

BIBLIOGRAPHY

- [1] "The What, Why and How of Wheel Balancing" (2014).
(tires.about.com/od/Tire_Safety_Maintenance/a/The-What-Why-And-How-Of-Wheel-Balancing.htm)
- [2] "Wheel Balancing" (2010).
(www.aa1car.com/library/wheel_balancing.htm)
- [3] The Pneumatic Tire, Published by NHTSA USDOT (2006).
- [4] Jerry M. Hill, Wheel balancing apparatus, US Patent 4046017, (1977).
- [5] "Principles of Tire and Wheel Balancing"
(<http://www.derekweaver.com/learn/wheel-balancer/>)
- [6] "Wheel weight Product Catalog" , (2011).
(http://www.perfectequipment.com/content/site/dateien/8625390811_pe_imagebrochure_sc)
- [7] Shelah Phillips, Wheel weight with body having recess and clip secured therein, US Patents 7216938 (2007).
- [8] Sanae Asayama, Koji Nakatsuji, Masanori Suzuki, Atsuhito Terao, "Radio-frequency receiver and integrated circuit for use in receiver", US Patent 7215938 (2007).
- [9] Chris C Zank, Phillip W. Snyder, Steven J. Schmidt, Shelah D. Phillips, Michael P. Astorino, "Wheel balancing weight with half-clip", US Patent 7249804 (2007).
- [10] Donald F. Dreher, Monterey Park, Calif, "Sponge rubber adhesive unit", US Patent 2292024 (1942).
- [11] Hubert D. Songer, "Wheel balancing weight", US Patent 3960409 (1976).
- [12] Michael T. Pursley, "Wheel balancing weight", US Patent 6364421 (1998).
- [13] Michael W. Douglas, "Wheel balancing apparatus and method", US Patent 5365786 (1994).
- [14] Dan Parker, Michael W. Douglas, "Wheel balancing apparatus and method with improved calibration and improved imbalance determination", US Patent 5396436 (1995).
- [15] Michael W. Douglas, "Wheel balancer quick calibration check", US Patent 5542294 (1996).
- [16] Karl Rothamel, "Apparatus and method for displaying unbalance of rotors during measurement", US Patent 4441355 (1984).

- [17] Richard A. Mitchell, Hoyt H. Nelson, Donald R. Sherman, "Self-calibrating data collection system for dynamic wheel balancing machine", US Patent 4250555 (1981).
- [18] Michael W. Douglas, "Split weight wheel balancing", US Patent 5355729 (1994).
- [19] "Hunter DSP9200 specification sheet" (2015).
(<http://www.hunter.com/Portals/0/Media/6354-T.pdf>)
- [20] "DSP9200 Series Wheel Balancer operating Instructions form 5473-T 01-10, Hunter Engineering Company, 2010. "
- [21] Michael W. Douglas, David M. Scribner, "Wheel balancer system with centering check", US Patent 6481282 (2002).
- [22] Taylor, John R. "An Introduction to Error Analysis: The Study of Uncertainties in Physical Measurements", University Science Books, (1982).
- [23] "Automotive Handbook", Robert Bosch GmbH, Chief editor: U. Adler (1986).
- [24] Jugal Papat, Aneesh Nabar, Meighan Read, Chen Fu, Chunhui Zhang, Galab Kausik, Harsh Patel, Peter Thomas Tkacik, "A Statistical Study of Tire Pressures on Road Going Vehicles", SAE international (2016).
- [25] "Variable friction arm W/Bracket," Manfrotto,
(<http://www.manfrotto.com/variable-friction-arm-w-bracke>) [Accessed 14 October 2015].